Charge transport in disordered materials

Simulations, theory, and numerical modeling
of hopping transport and
electron–hole recombination

Fredrik Jansson

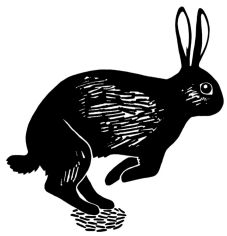

Physics
Center for Functional Materials
Graduate School of Materials Research
Department of Natural Sciences
Åbo Akademi University
Åbo 2011

Supervisor

Professor Ronald Österbacka
Åbo Akademi University

Pre-examiners

Professor Anders Sandvik
Boston University

Dr David Beljonne
University of Mons

Opponent for the public defense

Associate Professor Peter Bobbert
Eindhoven University of Technology

ISBN: 978-952-12-2610-6
Painosalama – Åbo 2011

Contents

Contents **iii**

Preface **vii**
Acknowledgments ix
List of included publications x
Author's contribution to the included articles xi

1 The hopping transport model **1**
1.1 The concept of sites 1
1.2 The hopping rate 2
1.3 Diffusion in the hopping transport model 5
1.4 Distribution of sites in space and energy 5
1.5 Parameters in the model 7
1.6 Applying the model—analytical and numerical approaches 8

2 Monte Carlo simulation of hopping transport **11**
2.1 The Monte Carlo method for a single electron 11
2.2 Simulating hops 12
2.3 Randomly placed sites 14
2.4 Hopping on a lattice 15
2.5 Relaxation 16
2.6 Simulation geometry 16
2.7 Eliminating soft pairs 18
2.8 Many-particle Monte Carlo simulation 20
2.9 Random numbers 23

3 Balance equations **25**
3.1 Linear balance equations 26
3.2 Solving the balance equations iteratively 28
3.3 Successive over-relaxation 29
3.4 Newton's method for balance equations 29
3.5 Solving the balance equations with Newton's method 30
3.6 Derrida's expressions for transport in one-dimensional systems . 32
3.7 Comparing numerical methods 35

4 Effective temperature for hopping transport **37**
4.1 Energy distribution of electrons at zero field 38
4.2 Energy distribution at non-zero field 39
4.3 Effective temperature for a Gaussian energy distribution 40
4.4 Further studies and conclusions 42

5 Negative differential conductivity **45**
5.1 Trapping and negative differential conductivity 46
5.2 Trapping at infinite field 47
5.3 Trapping at finite field 49
5.4 Simulation of the NDC effect 49
5.5 Coulomb blockade in the hopping transport model 51
5.6 Discussion 55

6 Diffusion in the hopping transport model **57**
6.1 General results on diffusion 59
6.2 Diffusion in one dimension 60
6.3 Diffusion in two and three dimensions 63
6.4 Multiple trapping 65
6.5 The sites that determine the diffusion coefficient 66
6.6 Why is the Einstein relation broken? 66

7 Recombination and diffusion **67**
7.1 Langevin's model 68
7.2 Recombination in two dimensions 69

Bibliography **73**

Svensk resumé **79**

Paper I
Effective temperature for hopping transport in a Gaussian DOS **81**

Paper II
Hopping conduction in strong electric fields:
Negative differential conductivity **91**

Paper III
Negative differential conductivity in the hopping transport model **105**

Paper IV
Effect of Electric Field on Diffusion in Disordered Materials
I. One-dimensional Hopping Transport **111**

Paper V
Effect of Electric Field on Diffusion in Disordered Materials
II. Two- and Three-dimensional Hopping Transport **125**

Paper VI
Role of Diffusion in Two-dimensional Bimolecular Recombination **139**

Preface

This thesis summarizes my research on charge transport in disordered materials. The work was done during the years 2007–2011 at the Physics department at Åbo Akademi University. I have worked in the Organic Electronics group, under the supervision of professor Ronald Österbacka. I have done my research in collaboration with professor Sergei Baranovskii at the University of Marburg, and Dr Alexey Nenashev from Novosibirsk State University.

The topic of my thesis is how electric current flows in a disordered material. This is an important problem for our research group, which investigates the possibilities of organic electronics. One aim of our group is to use organic materials for building electronic devices such as transistors, memories, light-emitting diodes and photovoltaics. Disorder in these materials plays an important role for their charge transport properties. In fact, disordered materials demand a completely different transport theory than the one developed for ordered materials, such as metals or crystalline semiconductors. Such a theory is provided by the hopping transport model, which I have used throughout this work. I have focused on modeling transport in the materials themselves, rather than trying to model complete devices. Once transport in the organic materials is understood, one can apply the knowledge to modeling whole devices built of these materials. This modeling in turn would help both in the interpretation of experimental results and in improving the device design.

The thesis is based on the six academic papers listed below. The selection of topics presented here is rather broad. We chose topics that we believed to be interesting theoretically as well as for experiments, while still being possible to study with the tools we had available. In the included papers both analytical and numerical calculations are presented. Since my contribution to the articles has mainly been numerical calculations, I emphasize the numerical methods in the introductory chapters. Chapter 1 describes the hopping transport model, which is the main building block of our studies. Chapters 2 and 3 present the numerical

methods that have been used in our work. Chapter 2 describes Monte Carlo simulation of hopping transport. Chapter 3 shows another approach, where the transport properties of a material is found by solving a system of equations, the balance equations obtained from the hopping transport model. The remaining chapters describe the six included papers.

The study of effective temperature, described in Chapter 4 and Paper I was my first chance to use the balance equation method for a numerical study of the hopping transport model. The main idea here is that the electric field and the temperature play similar roles for the hopping transport. For some purposes they can be combined into a single parameter, called the effective temperature. This combination leads to a simplified description of the charge transport process.

Papers II and III, described in Chapter 5, were inspired by experiments on organic memory devices done both by our group at Åbo Akademi and elsewhere. Simple memory devices can be constructed by placing small metallic particles in an insulating medium between two contacts. Among other effects, these devices show a so-called negative differential conductivity. This means that the current through the device decreases when the voltage over the device is increased. We wanted to investigate if this effect can be understood in the hopping transport model. As described in Chapter 5, there are two different ways in which this effect can appear in the model.

Papers IV and V, and Chapter 6, describe the random motion, or diffusion, of charge carriers in the hopping transport model. Specifically we studied how the diffusion coefficient depends on the electric field. We showed that the number of dimensions of the systems plays a crucial role for the behavior: in a one-dimensional system the diffusion coefficient appears proportional to the applied electric field, while the dependence in two and three dimensions is quadratic.

The diffusion theme is continued in Paper VI and Chapter 7, where we investigate the role of diffusion for the recombination of electrons and holes. Diffusion does not play any role in three dimensions, but becomes important when the charge carriers are constrained to move in only two dimensions. This is important for solar cells, where the recombination of electrons and holes decreases the device efficiency. The assumption of a two-dimensional material also has a practical relevance, since one of the polymers used in organic solar cells (P3HT, Poly(3-hexylthiophene)) forms layers, where the charge carriers can move much faster in two perpendicular directions than in the third one.

Acknowledgments

I am grateful to many people who have helped me in various ways during the time I have been working on this project.

In the Summer of 2007 I visited the University of Marburg, with the vague goal to learn something about charge transport in organic materials. Thanks to professor Peter Thomas, I ended up working with professor Sergei Baranovskii. Our collaboration resulted in Paper I. In 2008 I visited Marburg again, and had the fortune to meet and work with Dr Alexey Nenashev, who provided a different, analytical, point of view as a complement to my numerical work. Working with Sergei and Alexey has been a pleasure for me, and I have learned much from them. All articles included in this thesis are results of this collaboration. My supervisor, professor Ronald Österbacka, gave me much freedom in traveling and in research, and provided support and advice whenever I needed it. Thanks to Ronald and professor Markus Lindberg for initiating my visits to Marburg.

Associate Professor Peter Bobbert told me about the method of balance equations for studying hopping transport. This method is used in the first three articles included here. Ameya Joshi came to Turku as an exchange student in the Summer of 2008, and worked on numerical methods with me. He came up with the idea to solve the non-linear balance equations with Newton's method, which eventually led to the method presented in Section 3.4.

Dr Kaj Höglund kindly showed me the latex source code for his thesis. I gratefully inherited large parts of his document layout.

The heaviest computations were done at CSC—the Finnish IT center for Science. Dr Jan Åström helped me apply for an account at CSC and to get stated using the computers there. I want to thank Dr Kakhaber Jandieri, Dr Jacek Matulewski, Jan Oliver Oelerich, Dr Oleg Rubel, professor Boris Shklovskii, professor Peter Thomas, Maria Weseloh, and Martin Wiemer for discussing charge transport with me. My thanks also to everyone in the Physics department at Åbo Akademi, for making it such a nice place to work in. The same applies to the group of Vielteilchenphysik in Marburg, my thanks to all of you!

Johanna Grönqvist carefully read my text and helped me improve it and make it more friendly to the reader. She drew the final versions of the figures, and helped me typeset the text. My sincere thanks to her for this invaluable help and for everything else.

The Graduate School of Materials Research at Åbo Akademi and the International Research Training Group *Electron–Electron Interactions in Solids* (Marburg–Budapest) provided me with generous travel grants for visiting Marburg.

List of included publications

This thesis is based on the following six publications. The publications are reprinted here with permission from the publishers.

I. *Effective temperature for hopping transport in a Gaussian DOS*,
F. Jansson, S. D. Baranovskii, F. Gebhard, R. Österbacka,
Phys. Rev. B **77**, 195211 (2008)

II. *Hopping conduction in strong electric fields: Negative differential conductivity*,
A. V. Nenashev, F. Jansson, S. D. Baranovskii, R. Österbacka, A. V. Dvurechenskii, F. Gebhard,
Phys. Rev. B **78**, 165207 (2008)

III. *Negative differential conductivity in the hopping transport model*,
F. Jansson, A. V. Nenashev, S. D. Baranovskii, F. Gebhard, R. Österbacka,
Phys. Status Solidi A **207**, 613 (2010)

IV. *Effect of Electric Field on Diffusion in Disordered Materials I. One-dimensional Hopping Transport*
A. V. Nenashev, F. Jansson, S. D. Baranovskii, R. Österbacka, A. V. Dvurechenskii, F. Gebhard,
Phys. Rev. B **81**, 115203 (2010)

V. *Effect of Electric Field on Diffusion in Disordered Materials II. Two- and Three-dimensional Hopping Transport*,
A. V. Nenashev, F. Jansson, S. D. Baranovskii, R. Österbacka, A. V. Dvurechenskii, F. Gebhard,
Phys. Rev. B **81**, 115204 (2010)

VI. *Role of Diffusion in Two-dimensional Bimolecular Recombination*,
A. V. Nenashev, F. Jansson, S. D. Baranovskii, R. Österbacka, A. V. Dvurechenskii, F. Gebhard,
Appl. Phys. Lett. **96**, 213304 (2010)

Other related publications by the author, which are not part of this thesis, are given in the Bibliography, as references 1–8.

Author's contribution to the included articles

The articles included in this thesis were written in collaboration with the other co-authors, mainly Dr Alexey Nenashev and professor Sergei Baranovskii. In general, the analytical work was done by A. N., while the author was responsible for the numerical part of the studies. The author handled the submission to the journals and the correspondence with the editors.

The author implemented the numerical methods presented in Chapters 2 and 3 as a C program, and used this program to obtain the numerical results in Papers I–V. An exception is the simulations of infinite electric field in Paper II, which were done by A. N. For Paper VI, the author took part in the discussion and analysis, and in the writing of the final form of the text. The initial draft of the text was written by A. N., who also derived the equations presented in the paper.

Most of the numerical methods used in our work are well known in themselves, and references are given in the presentation below. However, the following methods appear to be new: solving the balance equations with Newton's method and sparse matrices (Section 3.4), the fast evaluation of Derrida's equation for drift and diffusion in a one-dimensional system (Section 3.6), and the fast implementation of Monte Carlo simulation on a lattice, described in Paper V.

Chapter 1

The hopping transport model

This chapter gives an overview of the hopping transport model, which is used throughout this work. The hopping transport model describes charge transport in a disordered material. It has been applied to amorphous inorganic semiconductors, such as amorphous silicon, and also to organic semiconductors such as π-conjugated polymers.

For a material to be conductive, it must contain some mobile charge carriers. In our materials, they are electrons or holes. We are interested in the movement of these charge carriers, typically in response to an electric field. The main quantity of interest is the charge carrier mobility μ, defined as the ratio of the average carrier velocity to the electric field F:

$$\mu = \langle v \rangle / F. \tag{1.1}$$

Frequently one is interested in how the mobility depends on the electric field F and the temperature T. Sometimes also the dependence on the concentration of charge carriers is studied. The average motion of the charge carriers subjected to an electric field is called drift. The mobility has a simple relationship to the current density j:

$$j = nq\mu F, \tag{1.2}$$

where n is the concentration of charge carriers and q is their charge.

1.1 The concept of sites

The defining property for the disordered materials we model is that they lack a crystal structure. In these materials, there are localized states for electrons

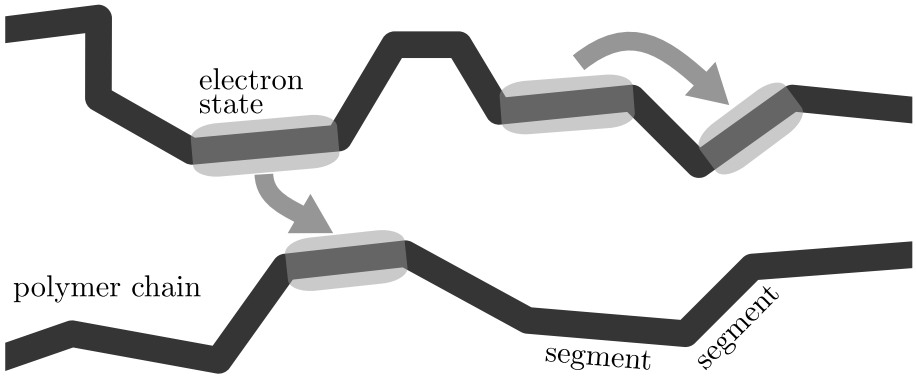

FIGURE 1.1 Hopping transport in a polymer. A charge carrier is localized to a straight segment of the polymer. It can move by hopping (tunneling) to another segment.

and holes. An electron might be confined to the vicinity of an impurity, to one molecule or to a segment of a conducting polymer, as illustrated in Fig. 1.1. Charge transport in this picture happens when the electrons or holes tunnel from one localized state to another. These tunneling events are the "hops" in "hopping transport". The states where electrons or holes can exist are called sites.

Charge carriers on different sites have slightly different energies, due to differences in their environments. In the case of polymers, the energy is also affected by the length of the polymer segment on which the carrier is localized [9].

1.2 The hopping rate

In the present model, it is assumed that the energy difference between the initial and final state in a tunneling event is taken care of by the emission or absorption of a phonon. As the probability to absorb a phonon of the correct energy depends on the temperature of the material, this assumption introduces a temperature dependence in the model. The transport properties of the material are determined by the rates of the different hopping events. The Miller–Abrahams hopping rate for phonon-assisted tunneling [10, 11] is frequently used, giving the rate of tunneling from a site i to a site j, located at a distance r_{ij} (see Fig. 1.2):

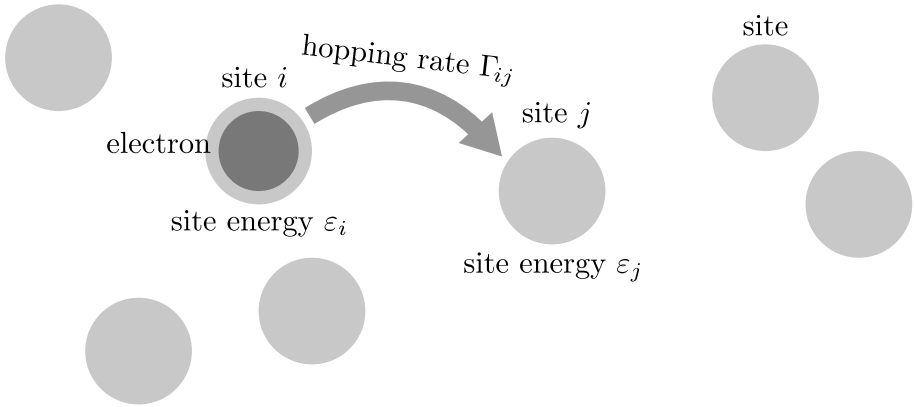

FIGURE 1.2 The hop from site i to site j. Site i has the energy ε_i, and the hopping rate is denoted Γ_{ij}.

$$\Gamma_{ij} = \nu_0 \, e^{-2\frac{r_{ij}}{a}} \begin{cases} e^{-\frac{\Delta\varepsilon_{ij}}{kT}} & \text{when } \Delta\varepsilon_{ij} > 0 \\ 1 & \text{when } \Delta\varepsilon_{ij} \leq 0 \end{cases}. \tag{1.3}$$

Here T is the temperature, k is the Boltzmann constant and ν_0 is the attempt-to-escape frequency. The localization length a describes the spatial size of the electron wave functions of the localized states, while $\Delta\varepsilon_{ij} = \varepsilon_j - \varepsilon_i$ is the difference in energy between the sites i and j. We see that the hopping rate between sites i and j depends exponentially on both their energy difference and on the distance between them. The factor $\exp(-\Delta\varepsilon_{ij}/kT)$ for jumps to a higher energy describes the probability of absorbing a phonon with the required energy. On the other hand, for jumps to lower energies it is assumed that a phonon taking away the excess energy can easily be emitted, this process has the weight 1 instead of the energy exponential.

For hopping in an electric field F as illustrated in Fig. 1.3, the field is taken into account in the energy difference. The energy difference between the sites i and j is then

$$\Delta\varepsilon_{ij} = \varepsilon_j - \varepsilon_i - Fe(x_j - x_i), \tag{1.4}$$

where ε_i is the energy of a charge carrier at site i, e is the elementary charge, and F is the magnitude of the electric field (which is assumed to be directed

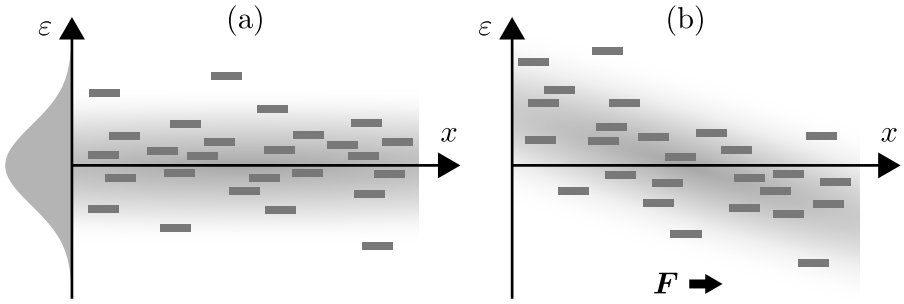

FIGURE 1.3 Distribution of sites in energy and one spatial coordinate. Figure (a) shows the case without an electric field. In Figure (b) an electric field is applied along the x direction, introducing a slope in the energy landscape.

along the x axis). The electric field, which we just introduced, creates a slope in the energy landscape. As the hopping rate Eq. (1.3) favors jumps to lower energies, the charge carriers will on average move along or against the field, depending on their charge. The mobility, introduced above, is a measure of the average drift speed.

In using the Miller–Abrahams rate, we assume that the sites have no structure. The hopping rate depends only on the distance between the sites. For a polymer such as the one illustrated in Fig. 1.1 this seems to be a very crude approximation, and it is known that the tunneling rate between organic molecules can be very sensitive to the relative orientation of the molecules [12]. However, in this way, one avoids the need for a detailed model of the polymer structure and the need to compute accurate hopping rates for different orientations, both of which are complicated tasks. It has been shown that already the simple model with the Miller–Abrahams hopping rate captures many of the features experimentally observed in conductive polymers and other disordered semiconductors [9, 13]. Another approximation is made in replacing the quantum-mechanical tunneling process by a classical random walk. This is justified when the tunneling rate is small, i.e. when the sites are far apart compared to the localization length. Further, we assume that no delocalized states, or bands, contribute to the transport. This assumption is generally made for disordered organic semiconductors [9, 13, 14]. In contrast, disordered inorganic semiconductors typically have conduction and valence bands, energetically above and below the localized states. In these systems, our assumption is valid if the temperature is so low, that the amount of charge carriers excited to the bands is negligible. Then tun-

neling between the localized states dominates the transport, and the hopping transport model described here is applicable. On the other hand, when the bands are important, the multiple-trapping model [15] is more appropriate.

To be specific I will assume that the charge carriers are electrons in all cases where only one species of charge carriers are present. Holes behave in the same way as far as the hopping transport model is concerned, except for the sign of the charge.

1.3 Diffusion in the hopping transport model

Besides the drift motion of the charge carriers, measured by the mobility, one can also measure their random motion, diffusion. The diffusion coefficient D measures how quickly a packet of charge carriers broadens:

$$D_x = \frac{\langle x^2 \rangle - \langle x \rangle^2}{2t}, \tag{1.5}$$

where the averages are taken over different electrons starting from the same position, after they have moved for the time t. For a two- or three-dimensional system in an electric field, the directions along the field and perpendicular to it are not equivalent. In this case, one can define separate diffusion coefficients for the two directions.

$$D_{||} = \frac{\langle x^2 \rangle - \langle x \rangle^2}{2t}, \qquad D_{\perp} = \frac{\langle y^2 \rangle + \langle z^2 \rangle}{4t}, \tag{1.6}$$

assuming a three-dimensional system with the electric field in the x-direction. The two diffusion coefficients are in general different. How diffusion in the hopping transport model depends on the applied electric field is the topic of Chapter 6.

1.4 Distribution of sites in space and energy

In order to use the hopping transport model, and for example calculate the mobility starting from the hopping rate (1.3), one would in principle need to know the positions and energies of all sites in the material. Since measuring this is impractical, one instead specifies only some statistics of how the sites are distributed in space and in energy. The energy distribution of the sites is described using the density of states $g(\varepsilon)$, defined so that $g(\varepsilon)d\varepsilon$ gives the concentration of sites with energies between ε and $\varepsilon + d\varepsilon$.

These distributions must be chosen according to the material one wishes to model. Since the hopping rate (1.3) has a strong, exponential, dependence on both the distance between the sites and on the energy difference between them, one would expect that the choice of distributions are decisive for the results obtained. The distribution of sites in energy and space is our main opportunity to adapt the hopping transport model to different types of materials.

For analytical work, it is often sufficient to know the statistics of site distribution, as given by the density of states $g(\varepsilon)$. In contrast, for numerical calculations one needs a specific system of sites, where the positions and energies of the sites are known. A straight-forward way to obtain such a system is to generate it randomly, in such a way that all statistical properties of the generated system obey what one knows about the material under study. The randomly generated system with specified properties is called a realization of the disorder.

It is common to assume that the sites are randomly distributed in space (with a uniform distribution). The negative differential conductivity effect, studied in Section 5.1, is a direct consequence of the random, uniform placement of sites in space. Another common approach is to place the sites on a lattice (a cubic lattice in three dimensions or a square lattice in two dimensions), since this permits the use of simple and efficient algorithms for computer simulations.

For the energy distribution of the sites, the two most popular assumptions are the exponential and the Gaussian distribution. In inorganic materials, an exponential density of states

$$g(\varepsilon) = \frac{N}{\varepsilon_0} \exp\left(\frac{\varepsilon}{\varepsilon_0}\right) \tag{1.7}$$

is usually assumed. Here N is the spatial density of sites while ε_0 gives the energy scale of the distribution. This choice is based on the shape of the optical absorption spectrum (the so-called Urbach tails) on one hand, and on the other hand on the agreement with experiments that is obtained when an exponential energy distribution is assumed in the hopping transport model.

For organic materials a Gaussian density of states is frequently used,

$$g(\varepsilon) = \frac{N}{\sigma\sqrt{2\pi}} \exp\left(-\frac{\varepsilon^2}{2\sigma^2}\right). \tag{1.8}$$

Here σ is the standard deviation of the distribution. There seems to be no rigorous justification for the use of a Gaussian distribution of site energies in organic materials [9]. The assumption of a Gaussian density of states is supported [9, 13, 14] by measurements of the absorption bands of organic semiconductors,

where a Gaussian shape is seen, and by the agreement of the predictions of the hopping transport model [13] with experimental results for organic materials. A Gaussian distribution of site energies is also to be expected, if the energy of one site is determined by many independent random contributions [9, 13]. In this work, a Gaussian energy distribution has been used, since we have been interested mostly in modeling organic materials.

It is simple to assume that the energies ε_i of different sites are independent of each other, i.e. not correlated. This assumption will be made throughout this work, unless explicitly stated otherwise. If the site energies depend on long-range effects, such as interaction with permanent electric dipoles or quadrupoles in the material, the energies of two spatially close sites will be correlated, since both sites have a similar environment. If such correlations are present, they may have a drastic effect on the transport properties of the material [16–19], as also seen in Paper I. The effects of space–energy correlations are briefly described in Paper I, with emphasis on the applicability of the effective temperature concept in the presence of correlations. In general, introducing correlations makes the energy landscape smoother, which increases the charge carrier mobility.

One further assumption that we have made is that the system of sites remains unchanged during the transport process. Organic materials are typically soft. Thus the structure of the molecules surrounding a site may change when an electron hops to that site. The electron, together with the distortion it creates, is then called a polaron. These structural changes affect the hopping rates in the system, since there is an energy associated with the deformation. The effects of the deformation can be taken into account by calculating the hopping rates using the Marcus theory [20], but will not be considered in this work.

1.5 Parameters in the model

The disorder strength, or disorder amplitude, is commonly specified by the standard deviation σ of the energy distribution. It is convenient to express temperature and electric fields compared to the disorder strength, using the dimensionless quantities kT/σ and eFd/σ, where $d = N^{-1/3}$. In the case of a lattice of sites, d gives the lattice constant, while d for randomly placed sites serves as a typical distance from a site to its closest neighbors. The localization length a can also be expressed as the dimensionless quantity a/d. For studying the dependence of the transport parameters on the amount of charge carriers present, one needs the additional parameter n, the (spatial) concentration of charge carriers.

With the definitions above, the task in the hopping transport model can be

stated more exactly: find the mobility μ and the diffusion coefficient D of charge carriers, as functions of

$$\frac{kT}{\sigma}, \quad \frac{eFd}{\sigma}, \quad \frac{a}{d}, \quad \text{and} \quad \frac{n}{N}.$$

The hopping rate (1.3) contains the constant ν_0, the frequency of jump attempts. This frequency is commonly assumed to be of the same order of magnitude as the phonon frequency of the material, around 10^{12} to 10^{14} s^{-1}. For simplicity, we will frequently state the results in units where $\nu_0 = 1$ and $d = 1$.

1.6 Applying the model—analytical and numerical approaches

The hopping transport process is controlled by both the energies of the sites and their placement in space. There is a trade-off between short jumps to the nearest neighbors and longer jumps to sites with lower energy. The length of the typical hops is determined by the parameters; a low temperature (in relation to the energetic disorder) and a long localization length (in relation to the site concentration) both make long jumps more favorable. This regime, where the hopping length varies with the temperature and localization length is called variable range hopping [21]. A different behavior appears when the temperature is high and the localization length is short. These conditions favor short jumps, and lead to hopping between nearest neighbors. The typical hopping length is then determined not by the temperature and localization length, but by the distances between the sites. This regime is called nearest-neighbor hopping.

A full analytical treatment of the hopping transport process has not been done. Particularly the case with a Gaussian density of states has resisted an analytical treatment. However, several important aspects of the model have been treated analytically. The case of hopping transport in a system of sites with equal energy in a small electric field, has successfully been analyzed with percolation theory. The mobility is seen to depend exponentially on the concentration of sites [21]. The temperature dependence of the mobility in the low-field limit has been understood in Vissenberg and Matter's extension of the percolation approach [22]. The temperature dependence of the mobility has also been analyzed using the concept of transport energy [23, 24]. With the transport energy approach, it has been shown that the low-field mobility depends on temperature according to

$$\ln(\mu) \propto -1/T^2, \tag{1.9}$$

for a Gaussian density of states, when the concentration of charge carriers is negligible. The transport energy treatment has recently been extended to account for the dependence of the transport energy level on the electron concentration [25]. The field-dependence of the mobility, however, is not easily obtained. One step in this direction is the effective-temperature idea presented in Chapter 4, but the problem is far from solved.

While general analytical solutions to the hopping transport problem are difficult to obtain, the problem is well suited for numerical solutions. Two popular numerical techniques are Monte Carlo simulation of the hopping process and solving balance equations relating the occupation probabilities of the sites and the flow of charge carriers between them. These methods are the topics of the two following chapters.

Chapter 2

Monte Carlo simulation of hopping transport

This chapter and the following one describe different methods used to calculate transport properties in the hopping transport model. Since the methods have their own strengths and weaknesses, they are suitable for different types of problems.

The most direct numerical approach to the hopping transport model is to simulate the motion of a single electron in a disordered system. The single-particle Monte Carlo method, which for many decades has been used to model hopping transport is described below, in Sections 2.1–2.5. Considerations of the choice of system geometry are given in Section 2.6. Section 2.7 describes how the simulation can be made more efficient, by a special treatment of fast back-and-forth jumps. The Monte Carlo method can also be extended to the case of many electrons hopping in the same system. This is the topic of Section 2.8. A few notes on the generation of random numbers are given in Section 2.9.

A different method to obtain numerical results in the hopping transport model is to determine the steady-state occupation probability for each site by solving a set of balance equations. This approach is described in Chapter 3.

2.1 The Monte Carlo method for a single electron

The first method used to study the hopping transport model numerically was Monte Carlo simulation [13, 26–29]. The simplest approach is to simulate one single electron at a time. This corresponds to such a low electron density that

interaction between electrons can be ignored.

The electron performs a random walk in the system of sites. We are interested in the statistics of this random walk. In the Monte Carlo method the transport parameters are determined by actually performing, with a computer program, such a random walk in a randomly generated system of sites. For each hop that the electron makes in the simulation, the destination site is chosen randomly, but weighted by the hopping rates to each possible destination site. The time the carrier spends on each site is also chosen randomly, and depends on the total rate of hopping out of that site [13, 28, 29]. After many jumps, one collects statistics of the electron's motion, and can then determine the transport properties of the material.

The Monte Carlo method is relatively simple to implement, especially for a system where the sites are placed on a lattice. Of all the methods presented here, Monte Carlo simulation on a lattice of sites can be implemented with the least amount of computer memory per site. Thus Monte Carlo is a good choice when one needs to simulate extremely large systems. I have used Monte Carlo simulation to study charge carrier diffusion in Paper V, and also as verification for the other methods. Let us now continue with a more detailed description of the simulation, first of how the hops are performed, then of how the system of sites is generated. The system generation part is common to all simulation methods considered, and is applicable also in the next chapter.

2.2 Simulating hops

When the electron is located at site i, the probability that the next jump takes it to the site j is given by

$$p_{ij} = \frac{\Gamma_{ij}}{\Gamma_i}, \tag{2.1}$$

where Γ_{ij} is hopping rate from site i to j and Γ_i is the total rate of hopping away from site i,

$$\Gamma_i = \sum_j \Gamma_{ij}. \tag{2.2}$$

The time τ that the electron spends on the site i before hopping, (the "dwell time") is calculated as

$$\tau = T/\Gamma_i, \tag{2.3}$$

FIGURE 2.1 A destination site is selected by picking a random number x, and finding the interval in which it falls. The destination site corresponding to that interval is selected, in this case site 5.

where T for each hop is randomly generated with an exponential distribution with unit expectation value and unit variance. Thus τ has an exponential distribution, with the expected value $1/\Gamma_i$. Which jump to perform is decided by picking a random number x between 0 and 1 from a uniform distribution, and finding j such that

$$\sum_{k=1}^{j-1} p_{ik} \leq x < \sum_{k=1}^{j} p_{ik}. \tag{2.4}$$

This selection procedure is illustrated in Fig. 2.1. It ensures that when the electron jumps from site i, each site j is selected with the probability p_{ij}. In the context of simulating chemical reactions, this method is known as the Gillespie algorithm [30, 31]. In practice only the right-hand inequality needs to be tested. One starts from $k = 1$ and adds one term at a time to the sum, stopping as soon as the sum exceeds x.

The program places an electron at a randomly chosen starting site, and simulates its trajectory during a fixed simulation time t_s. In order to simulate the transport properties of an infinite system, periodic boundary conditions are applied in all directions, Fig. 2.2. The process is then repeated for the next electron, until enough statistics has been collected. The mobility is calculated as

$$\mu = \frac{\langle x \rangle}{F t_\mathrm{s}}, \tag{2.5}$$

while the diffusion coefficient parallel and perpendicular to the field are

$$D_{||} = \frac{\langle x^2 \rangle - \langle x \rangle^2}{2t_\mathrm{s}}, \qquad D_\perp = \frac{\langle y^2 \rangle + \langle z^2 \rangle}{4t_\mathrm{s}}, \tag{2.6}$$

assuming a three-dimensional system with the electric field in the x-direction.

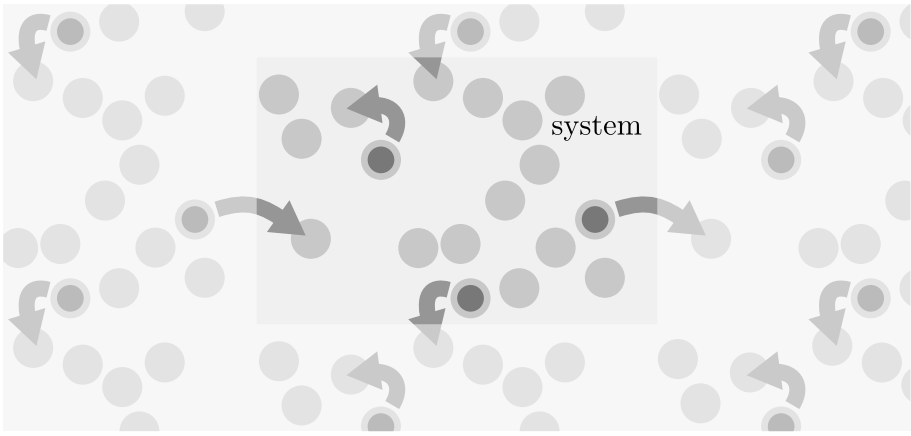

FIGURE 2.2 Periodic boundary conditions. An electron can leave the system by moving over its border, and will then enter the system again at the opposite side.

2.3 Randomly placed sites

The program generates the system to study by placing sites either on a lattice or randomly in space, and choosing energies for them according to some specified distribution, typically Gaussian or exponential. If one wants to study a system with correlated disorder (as in Paper I), the correlations have to be generated at this stage. We will here consider the general case where the sites are randomly placed in the simulation volume. The special case of sites on a lattice permits some optimizations, discussed below in Section 2.4.

In principle, arbitrarily long hops are possible in our model. But since the hopping rate (1.3) decreases exponentially with the distance, it is a good approximation to allow only jumps shorter than some cut-off length r_{cut}. This limits the number of paths an electron can take from a given site.

When selecting a jump, one needs an efficient way to find the possible target sites to choose from. I have chosen to store a list of neighbors for each site, and the hopping rate to each of these neighbor sites. The total rate Γ_i for hopping away from each site i is also stored. The simulation is efficient, since when choosing which jump to perform all the needed quantities can be found in the lists. Keeping only the jumps shorter than the cut-off length is important here, since it decreases the amount of memory needed to store the neighbor lists.

The neighbor lists can be created efficiently with the so-called linked cell

method [32]. In order to speed up the jump selection process, i.e. the search for the j that satisfies Eq. (2.4), the neighbor lists should be sorted in order of decreasing rates. In this way, the average number of terms needed in the sum (2.4) is kept small.

2.4 Hopping on a lattice

When the sites are placed on a lattice it is convenient to store the site energies in an array. The site coordinates do not need to be stored explicitly, as they can be calculated on the fly from the site's position in the array. Because of the regular geometry of a lattice, the hopping rates can be calculated very efficiently, see the appendix of Paper V for a description of our method for this case. The lattice Monte Carlo method also consumes very little memory for each site. In our implementation we store only the site energy ε_i and the total rate for leaving site, Γ_i for each site i. (Actually, to avoid calculating exponentials during the hopping stage, we store $\exp(\varepsilon_i/kT)$ instead of ε_i.) The individual jumping rates are then calculated as they are needed while evaluating Eq. (2.4). By considering short jumps before long ones in the sum (2.4), the number of terms needed is kept small on average.

For randomly placed sites, the hopping rates to neighbor sites were stored in lists. Then, the periodic boundary conditions had to be considered only when generating these lists. Now, we want to calculate the hopping rates during the simulation in order to save memory, and when doing so, the periodic boundary conditions must be observed. The periodic boundary conditions can be implemented with a modulo operation. Let the site energies be given by $\varepsilon(x, y, z)$, where x, y, and z are integers and $0 \leq x, y, z < L$. One can then make the material periodic by writing the site energies as

$$\varepsilon(x, y, z) = \varepsilon(x \bmod L, y \bmod L, z \bmod L) \tag{2.7}$$

and dropping the restrictions on the coordinates. This approach is simple in principle, but results in a poor performance since the modulo operation is slow. If the system size L is chosen as a power of 2, one can replace the modulo with a much faster binary AND operation: $x \bmod L$ is replaced by x AND $(L-1)$. I chose instead to compare each coordinate with 0 and L, and to move each coordinate inside the system, whenever it would move over a border. Further, the ε-array was extended in each direction by the cut-off length, so that no comparisons are needed when choosing a destination, but only when actually moving the electron.

The use of helical boundary conditions [33] instead of the regular periodic ones can further increase the efficiency. With this approach, the indexing and the boundary conditions are written in a compact and efficient way. However, the system geometry becomes more complicated since the simulation volume is no longer a cube.

Does it matter whether one places the sites randomly or on a lattice? The answer is that it depends—in Paper I, Fig. 7 the mobility differs roughly 10 % between a lattice and a random system (without correlations), while the whole negative differential conductivity effect studied in Paper II comes from the random site placement.

2.5 Relaxation

When placing electrons at randomly chosen sites, their energy distribution will be that of the sites. With time, they move to sites with lower energies. This *relaxation* process depends on the energy distribution of the sites, temperature and the electric field [13]. While the electrons move downwards in energy their mobility decreases, and approaches the steady state value. To obtain steady-state values for the diffusion coefficient and the mobility, one should let the electrons relax for some time t_{relax} before starting to collect data about the transport. (This is valid with a Gaussian density of states, where a steady state exists and one can determine an equilibrium energy for a single electron [13]. For an exponential density of states there is no steady state for a single electron moving in an otherwise empty system.)

2.6 Simulation geometry

The early Monte Carlo hopping simulations by Bässler et al. were typically performed on a finite system. The electrons were started at one border of the system, and the simulation was continued until they arrived at the opposite border [13]. This setup corresponds closely to a time-of-flight experiment, and much understanding of time-of-flight results has been gained from simulations of this kind.

However, there are two problems in this approach, if one is interested in properties of the material that are independent of any particular device structure. For example, the steady state electron mobility is such a property. The first problem is the relaxation described above. When the electrons are injected

into the system, they have the same energy distribution as the sites. Then as they move through the system they also relax towards their equilibrium energy. If the time to relax is comparable to the time it takes for the electrons to cross the sample, the transport velocity that one measures will depend on the sample thickness. This is known as dispersive transport. Dispersive transport is observed in time-of-flight experiments, and in general is more pronounced for low temperatures and thin samples. However, if one is interested in the steady state mobility as a material property, the dispersive transport is an added complication.

The second problem is that the time it takes for an electron to cross a finite sample is affected not only by electron drift but also by diffusion. For example, in the case of no applied field, if an electron is injected at one side of a finite sample, it will sooner or later emerge at the opposite side due to its random, diffusive motion. One should not attribute this transit time to the electron's drift velocity. At large electric fields the time to cross a sample of thickness d, the transit time t_{tr}, is determined mainly by the electron drift velocity. Then the mobility μ can be determined as

$$\mu = \frac{\langle v \rangle}{F} = \frac{d}{t_{\mathrm{tr}} F}. \tag{2.8}$$

In the limit of small electric fields the transit time is determined by electron diffusion. If one tries to determine the mobility μ using the drift formula at such small fields, one obtains a mobility that decreases with increasing electric field F, just because F appears in the denominator. If one instead accounts for both drift and diffusion [34, 35], the mobility turns out to be independent of the field strength at low fields.

These difficulties can be avoided by considering a material without boundaries (by periodic boundary conditions, as described above), and by running the simulation for a fixed simulation time instead of waiting for the electrons to travel a fixed distance. Furthermore, one can let the electrons relax for some time t_{relax} before starting to collect data. In a infinite (or at least borderless) system, diffusion and drift are clearly distinguishable, and diffusion will not affect the average velocity $\langle v \rangle$. Thus the mobility is correctly given by $\mu = \langle v \rangle / F$ in this case. In our bulk calculations the mobility is seen to be constant at low electric fields and then to increase with the field at higher fields, see for example Fig. 1 in Paper V.

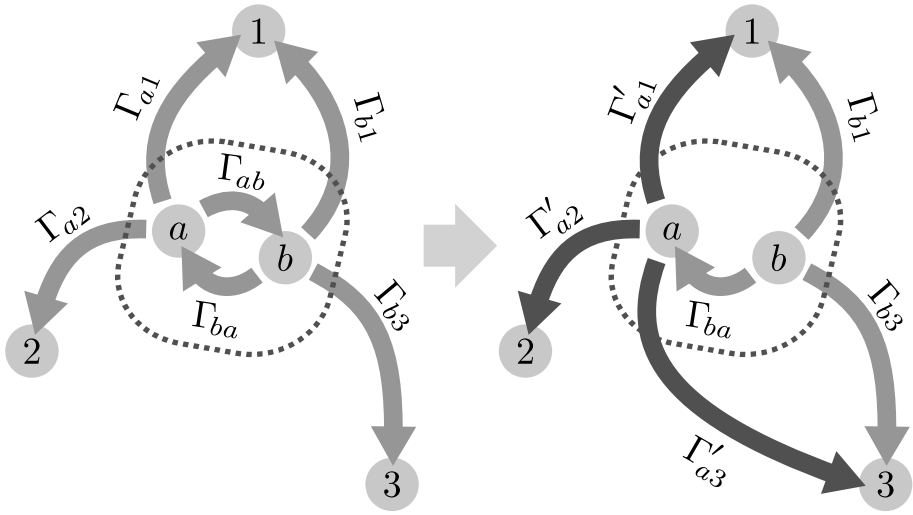

FIGURE 2.3 The sites a and b form a soft pair. The transition from a to b is removed, and the other rates from a are modified to compensate. Rates that are not involved in the soft-pair calculation are omitted for clarity.

2.7 Eliminating soft pairs

A technical difficulty that can arise in the Monte Carlo simulation is the problem of so-called soft pairs. If two sites are spatially close and have energies near each other (relative to kT), the jump rates between these sites will be high in both directions. Then an electron that arrives at one of these sites may jump back and forth a large number of times before escaping the pair of sites. This configuration of sites is known as a soft pair. Soft pairs make the simulation inefficient, since each simulation step where the electron hops between the two sites advances the simulation time by only a small amount. The problem of soft pairs is most severe when simulating systems with randomly placed sites and when the localization length is small.

The soft pairs can be eliminated with the following method, adapted from a technique given by Ortuño et al. for efficient simulation of the Coulomb glass [36, 37]. Consider the pair of sites a and b shown in Fig. 2.3. An electron on site a can arrive at some other site x in several ways: directly with the probability p_{ax}, via site b with the probability $p_{ab}p_{bx}$, first to b, then back to a, then to x, and so on. We will now modify the hopping rates in the vicinity of the soft pair,

to eliminate the transition from a to b, but to preserve rates of escaping the pair. In doing so we change the local properties of the system to make the simulation more efficient, in a way that preserves the global transport properties.

The following is a derivation of the rate Γ'_{ax} for the electron to arrive at the site x after any number of jumps back and forth between the sites a and b. The final result is given in Eq. (2.13). Let p_{ax} denote the probability that an electron on site a hops to site x in its next hop. Then,

$$p_{ab} = \Gamma_{ab}/\Gamma_a = \Gamma_{ab}\tau_a. \tag{2.9}$$

The probability that the electron hops to site x when it leaves the pair, if it starts at site a (after any number of jumps inside the pair) is

$$\begin{aligned} p'_{ax} &= p_{ax} + p_{ab}p_{bx} + p_{ab}p_{ba}p_{ax} + \dots \\ &= \frac{p_{ax} + p_{ab}p_{bx}}{1 - p_{ab}p_{ba}} = \frac{\Gamma_b\Gamma_{ax} + \Gamma_{bx}\Gamma_{ab}}{\Gamma_b\Gamma_a - \Gamma_{ab}\Gamma_{ba}}, \end{aligned} \tag{2.10}$$

where Eq. (2.9) was used in the last step. The expectation value of the time to leave the pair, when starting from a is

$$\begin{aligned} \tau'_a =& \tau_a(1 - p_{ab}) + (\tau_a + \tau_b)p_{ab}(1 - p_{ba}) \\ &+ (\tau_a + \tau_b + \tau_a)p_{ab}p_{ba}(1 - p_{ab}) + \dots \\ =& \frac{\tau_a + \tau_b p_{ab}}{1 - p_{ab}p_{ba}}. \end{aligned} \tag{2.11}$$

The rate of escaping the pair, starting from a is now

$$\Gamma'_a = \frac{1}{\tau'_a} = \frac{\Gamma_a\Gamma_b - \Gamma_{ab}\Gamma_{ba}}{\Gamma_b + \Gamma_{ab}}, \tag{2.12}$$

where Eq. (2.9) again gave the last step. Finally we use Eqs. (2.10) and (2.12) to obtain the rate of escaping the pair to site x

$$\Gamma'_{ax} = p'_{ax}\Gamma'_a = \frac{\Gamma_b\Gamma_{ax} + \Gamma_{bx}\Gamma_{ab}}{\Gamma_b + \Gamma_{ab}} \tag{2.13}$$

The procedure to eliminate the transition from a to b is then to replace all transition rates Γ_{ax} by Γ'_{ax} given in Eq. (2.13) for each site x within the distance r_{cut} of site a or b, and then set $\Gamma_{ab} = 0$.

A way to verify the soft-pair elimination algorithm is to determine the mobility in the same test system by the balance equation method (Chapter 3) with

and without performing the soft-pairs elimination. The results should be identical. Using the balance equation method eliminates the problem of noise that would be present in two different Monte Carlo runs.

In the derivation above, we assumed that there is at most one particle present inside the pair. For example, when site a is occupied, site b is assumed to be empty. In a many-particle simulation, this assumption is not necessarily true, so the result derived above is valid only for single-particle simulations. For many-particle work, the original method of Ortuño et al. [36, 37] is more suitable. That method considers transitions not of electrons between individual sites but of the whole system from one configuration to another.

2.8 Many-particle Monte Carlo simulation

The Monte Carlo method described in the previous section can be generalized to treat many electrons hopping in the same system. It is then possible to study the effects of interaction between the electrons. Simulating many electrons simultaneously gives the possibility to see how the transport properties depend on the electron concentration.

Two kinds of interaction have in general been considered: Pauli exclusion [38], i.e. that each site can accept at most one electron, and Pauli exclusion together with Coulomb interaction [39–41]. Also the Coulomb glass model [21, 42] has been extensively studied using many-particle Monte Carlo methods [43]. We used many-particle simulation in the study of negative differential conductivity (Chapter 5), both in the model with geometric traps (Paper II) and in the model with Coulomb blockade effects (Paper III).

Exclusion effects can be studied with the balance equation method presented in the next chapter. When Coulomb interactions are included, it is not clear that the mean-field approximation used in the balance equations is valid. However such mean-field calculations have been made for the Coulomb glass [44]. The many-particle Monte Carlo method is simple in principle, and serves as a good reference with which to compare the balance equation method, for example to judge the effects of the mean-field approximation made there. An efficient implementation of the many-particle simulation is more difficult than in the single particle case presented above, since the set of allowed jumps change during the simulation. If Coulomb interactions are taken into account, the site energies change as well. A few different approaches are briefly described below, first for the case of only exclusion and then for the Coulomb interaction case.

Many particles with Pauli exclusion

For simulating many particles, without Coulomb interaction, there are two different approaches. Gillespie [30, 31] calls them the direct method and the first reaction method.

In the direct method, one randomly selects one of the jumps that are possible in the current configuration, and performs it. The selection is in principle similar to the one-particle case described above, in Section 2.2. An electron can only jump to unoccupied sites. This means, that the set of possible jumps in the system depends on the position of all electrons. To efficiently select one of the allowed jumps, the jumps can be organized in a binary tree [45, 46]. With the tree, one can efficiently keep track of which jumps are allowed and which are forbidden at each step. The tree-method was used for the many-particle simulations in Paper II.

In the first reaction method, one randomly chooses a time for each of the allowed jumps to occur. The jumps are then ordered in some form of queue structure, such as a heap or priority queue. The jumps are performed in sequence, always taking the one with the earliest time. When one jump is performed, it causes some previously forbidden jumps to be allowed. These new jumps must be assigned times and be inserted in the table of future events. Also, some of the allowed jumps will become forbidden, and should be deleted from the event queue. Lukkien et al. [47] describe how to handle this rather complex book-keeping efficiently. The many-particle hopping problem is very similar to simulating the kinetics of chemical reaction systems. In fact, the references given above are all from this field.

Finally, there is one more algorithm, free from the book-keeping problems outlined above. The algorithm is a variant of the direct method, and is based on the accept/reject technique [43]. In each simulation step, select one pair of sites. Each pair (i, j) is selected with a probability proportional to the hopping rate Γ_{ij}, without regarding whether the sites are occupied or not. The probability to select the pair (i, j) is

$$p_{ij} = \frac{\Gamma_{ij}}{\sum_{m,n \neq m} \Gamma_{mn}}. \tag{2.14}$$

Once the pair (i, j) is selected, test if site i is occupied and site j is empty. If so, the pair is accepted and the electron is moved from site i to j, otherwise the

pair is rejected. Each jump attempt corresponds to the physical time

$$\Delta t = \frac{1}{\sum_{m,n\neq m} \Gamma_{mn}}, \tag{2.15}$$

regardless of whether the jump is accepted or not.

The set of jumps to select from, and the selection probabilities, stay constant during the simulation. The jumps can be selected without regarding whether the sites are occupied or not, since the accept/reject step takes care of the site occupation. For this reason, Walker's efficient method of aliases [48–50] can be used to perform the selection. The computational effort in selecting one pair is extremely small: two random integers, one or two table look-ups, one shift, and one comparison is all that is needed. How the method performs in practice depends on the fraction of rejected jumps. This method is at its most efficient when close to one half of the sites are occupied. Significantly lower or higher occupations will most probably lead to a higher fraction of rejected jumps.

Many particles with Coulomb interaction

When Coulomb interaction between the electrons are considered, in addition to the exclusion effect discussed above, the simulation becomes more complicated and in general more time consuming. All site energies change when one electron is moved, and thus all hopping rates also change after each jump. For this reason some variant of the direct method seems most promising. A variant of the first reaction method has also been used [41], but here all future jumps in the queue have to be updated after each jump that is made.

Tsigankov et al. [43] give an efficient method for simulating hopping with Coulomb interaction. It uses the direct method to select a jump based on the jump length, and then accepts or rejects that jump based on the change in energy. The reason for this division is that the lengths of the jumps stay constant during the simulation, while the site energies fluctuate. By treating the changing quantities in the accept/reject step, the selection step is kept simple and efficient. Furthermore, one avoids calculating the energy-dependent hopping rates for all transitions in the system, since the energy change is needed only in the accept/reject step.

For selecting the candidate pair (i, j), the binary tree method or Walker's alias method can be used. The tree method generates only allowed transitions, i.e. transitions where the starting site is occupied and the destination site is

empty. The alias method chooses without regarding site occupation, so the occupation must be considered in the accept/reject step. We used Tsigankov's method for simulating hopping with Coulomb interaction in Paper III. The candidate pairs were chosen with the binary tree method.

2.9 Random numbers

The simulation uses random numbers in two different steps: first in generating the system of sites, and then in choosing the paths that the electrons take through that system. It is important to use random numbers of a high quality, although a precise definition of high quality for computer-generated random numbers is difficult to give [50]. Any irregularities, such as correlations between successive random numbers, might distort the results. In particular, the random number generators of the C standard library have a bad reputation for simulations [51]. In my simulation, I have generated the random numbers with the Mersenne Twister algorithm [52]. For site energies and for dwell times, random numbers with specified distributions are required, typically exponential and Gaussian distributions. Methods for generating these numbers are given in Refs. 32 and 50.

Chapter 3

Balance equations

In the previous chapter it was shown how the transport properties of a disordered material could be determined from the statistics of simulated electron trajectories. In this chapter, a different approach is described, where one does not follow individual particles, but instead considers the probability p_i for each site i to be occupied in the steady state. The current in the system and the electron mobility are then determined from the occupation probabilities. As in the previous chapter, we consider a system with periodic boundary conditions. An electron leaving the system at one border enters the system at the opposite border. For this reason it is possible to have a current in the steady state.

The occupation probabilities are determined by solving a set of balance equations, also known as the master equation. These equations relate the occupation probabilities of the sites and the electron flow between the sites in the steady state. The flow of electrons from site i to site j can be expressed in terms of the occupation probabilities as $p_i\Gamma_{ij}(1-p_j)$. The electron flow, i.e. the number of electrons undergoing this transition per unit of time, is given by the transition rate Γ_{ij} weighted by the probability that the starting site is occupied and that the destination site is empty. Here we have made an important assumption, known as the mean-field approximation, that the site occupations are independent of each other. In this approximation, the state of the system can be fully described by specifying the occupation probability of each site. We will now search for the occupation probabilities for the steady state.

In the steady state, all occupation probabilities are constant in time and the total flow of probability into each site equals the flow out of that site. In the

mean-field approximation the balance equation has the form [53–56]

$$\sum_{j\neq i} p_i \Gamma_{ij}(1-p_j) = \sum_{j\neq i} p_j \Gamma_{ji}(1-p_i). \tag{3.1}$$

This is a system of non-linear equations, one equation for each site. The main topic of this chapter is to solve this system of equations efficiently in different cases.

Once the occupation probabilities p_i are determined, the average drift velocity of the electrons is given by

$$\langle v_x \rangle = \sum_{i,j\neq i} p_i \Gamma_{ij}(1-p_j)(x_j - x_i) \Big/ \sum_i p_i, \tag{3.2}$$

and the mobility is again $\mu = \langle v_x \rangle / F$.

In the limit of low concentrations, the equations can be linearized and efficiently solved with linear algebra methods, as shown in Section 3.1. At finite concentrations on the other hand, when non-linear effects are important, one has to solve the full non-linear system of equations (3.1). This more difficult problem can be solved with an iterative procedure given by Yu et al. [53–56], which is described in Section 3.2, or by applying Newton's method as described in Sections 3.4 and 3.5. An efficient numerical method for the special case of one-dimensional systems is presented in Section 3.6. The chapter is concluded with a discussion of the strengths and weaknesses of all the numerical methods, in Section 3.7.

The balance equation method was used in Paper I (non-linear method) and II (linear method), where we were interested explicitly in the site occupation probabilities. The one-dimensional method was used in Paper IV for studying the diffusion of electrons in a chain of sites.

3.1 Linear balance equations

In the limit of low concentration, when all $p_i \ll 1$, Eq. (3.1) can be linearized [57] to

$$\sum_{j\neq i} p_i \Gamma_{ij} = \sum_{j\neq i} p_j \Gamma_{ji}, \tag{3.3}$$

For one particle hopping in an otherwise empty system this equation is exact, otherwise it is an approximation. Eq. (3.3) expressed in matrix form is $\boldsymbol{M}\boldsymbol{p} = 0$,

where

$$\boldsymbol{p} = \begin{pmatrix} p_1 \\ p_2 \\ p_3 \\ \vdots \end{pmatrix} \text{ and } \boldsymbol{M} = \begin{pmatrix} -\Gamma_1 & \Gamma_{21} & \Gamma_{31} & \cdots \\ \Gamma_{12} & -\Gamma_2 & \Gamma_{32} & \cdots \\ \Gamma_{13} & \Gamma_{23} & -\Gamma_3 & \cdots \\ \vdots & \vdots & \vdots & \ddots \end{pmatrix}. \tag{3.4}$$

The diagonal elements $\Gamma_i = \sum_{j \neq i} \Gamma_{ij}$ give the total rate of jumping out of each site i. The matrix $\boldsymbol{M}$ defined above is singular. If any one of the balance equations is replaced by the normalization condition

$$\sum_i p_i = 1, \tag{3.5}$$

the matrix becomes non-singular.[1] The equation defining $\boldsymbol{p}$ now reads

$$\begin{pmatrix} 1 & 1 & 1 & \cdots \\ \Gamma_{12} & -\Gamma_2 & \Gamma_{32} & \cdots \\ \Gamma_{13} & \Gamma_{23} & -\Gamma_3 & \cdots \\ \vdots & \vdots & \vdots & \ddots \end{pmatrix} \begin{pmatrix} p_1 \\ p_2 \\ p_3 \\ \vdots \end{pmatrix} = \begin{pmatrix} 1 \\ 0 \\ 0 \\ \vdots \end{pmatrix}. \tag{3.6}$$

The problem is easier to solve in this form, and the solution is automatically normalized.

Since the hopping rate quickly decreases with increasing hopping distance, it is a good approximation to ignore jumps longer than a cut-off length r_{cut} by setting $\Gamma_{ij} = 0$ when $r_{ij} > r_{\text{cut}}$. Then a sparse storage scheme can be used, where only the non-zero matrix elements are stored, leading to reduced memory demands for the algorithm. I have used GNU Octave and Matlab for solving sparse versions of Eq. (3.6).

Once the site occupation probabilities p_i are known, the average electron velocity along the field and the mobility can be determined as

$$\langle v_x \rangle = \sum_{i,j \neq i} p_i \Gamma_{ij} (x_j - x_i), \qquad \mu = \frac{\langle v_x \rangle}{F}. \tag{3.7}$$

Compared to the Monte Carlo method, the linear balance equation method is more efficient, and guarantees a steady state result. The price for these advantages is a higher memory consumption than with the Monte Carlo method, even when using sparse matrices.

[1] suggested by Dr Alexey Nenashev

The linear balance equations considered here can be used for any field strength, but only in the limit of a low electron concentration. Pasveer et al. [58] takes the approach to linearize the balance equation (3.1) around the zero-field occupations given by Fermi–Dirac statistics (see Eq. (4.4) in Chapter 4). In this way, the linear equations are valid for finite concentrations, but in the limit of small electric field.

The linear method forms the basis for Newton's method presented in Section 3.4, where the non-linear balance equations are linearized around an estimate of the solution. Solving the linearized equation then gives an improved estimate. This process is repeated until a solution with sufficient accuracy is obtained.

3.2 Solving the balance equations iteratively

The non-linear balance equation (3.1) can be solved with an iterative method described by Yu et al. [53, 54]. The procedure was further used and discussed by Pasveer et al. [55] and Cottaar and Bobbert [56]. In the iterative solution procedure, the balance equation (3.1) is rewritten in the form

$$p_i = \frac{\sum_{j \neq i} \Gamma_{ji} p_j}{\sum_{j \neq i} \Gamma_{ij} - \sum_{j \neq i} (\Gamma_{ij} - \Gamma_{ji}) p_j}, \tag{3.8}$$

where p_i appears only on the left-hand side. The procedure starts by initializing all p_i to some starting values, for instance the zero-field solution given by Fermi–Dirac statistics (4.4). This solution is improved in steps, by sequentially using Eq. (3.8) to determine one p_i at a time from all the other p:s. This procedure is repeated until the solution has reached a sufficient accuracy. The value p_i is updated immediately when it has been calculated, so that the new value is used in all subsequent calculations. This so-called implicit iteration is necessary for obtaining convergence [54]. At least for linear systems, this method is also known as Gauss–Seidel iteration [51]. A difficulty with this procedure is that replacing p_i by the value calculated in Eq. (3.8) does not conserve the total number of charge carriers. Thus, if one wishes to obtain a solution with a specified amount of electrons, one must periodically scale all p_i so that the total amount of electrons is correct [56]. Here, as in the other methods, one can set $\Gamma_{ij} = 0$ when r_{ij} is larger than some cut-off length r_{cut}.

3.3 Successive over-relaxation

Another idea that can be borrowed from the field of iterative methods for linear problems is the method of successive over-relaxation (SOR). Using SOR gives a faster convergence of the calculation. In this method, the iteration is carried out as described above, but the new value p_i'' for the occupation probability of site i is given by

$$p_i'' = \omega(p_i' - p_i) + p_i \tag{3.9}$$

where p_i' is calculated using Eq. (3.8), p_i is the old value of the occupation probability, and ω is a constant. Setting $\omega = 1$ gives the Gauss–Seidel iteration, while using $\omega > 1$ amplifies the changes in each step which can lead to a faster convergence. For linear systems it can be shown that the iteration always converges for $0 < \omega < 2$, and some theory for choosing the optimal ω exist [51]. In the non-linear case, choosing ω too large leads to divergent behavior, even for $\omega < 2$, and the best ω has to be found by trial and error. Even so, using SOR can reduce the computational effort needed by several times.

3.4 Newton's method for balance equations

A different way to solve the system of non-linear equations (3.1) is to apply Newton's method [51]. This is equivalent to linearizing the system of equations, but not around $p = 0$ as in the low concentration case above, but around the current estimate of the solution.[2] Successively better estimate of the solution are then obtained by repeatedly solving the linear system of equations. Briefly, Newton's method finds the vector $\boldsymbol{p}$ such that

$$\boldsymbol{f}(\boldsymbol{p}) = \boldsymbol{0}, \tag{3.10}$$

where $\boldsymbol{f}(\boldsymbol{p})$ is a vector of functions, $f_1, f_2, \ldots$. If the current estimate of the solution is $\boldsymbol{p}$, a correction $\delta\boldsymbol{p}$ to the estimate is obtained by solving

$$\boldsymbol{J}\delta\boldsymbol{p} = -\boldsymbol{f}(\boldsymbol{p}), \tag{3.11}$$

where $\boldsymbol{J}$ is the Jacobian matrix, and the improved estimate of the solution is then $\boldsymbol{p}_{\text{new}} = \boldsymbol{p} + \delta\boldsymbol{p}$ [51]. To apply Newton's method on the balance equations (3.1), we define

$$f_i(\boldsymbol{p}) = \sum_j p_i\Gamma_{ij}(1 - p_j) - p_j\Gamma_{ji}(1 - p_i), \tag{3.12}$$

[2] first suggested to me and implemented by Ameya Joshi

where we for convenience choose $\Gamma_{jj} = 0$. The balance equations are now in the form of Eq. (3.10). The elements of the Jacobian matrix $\boldsymbol{J}$ are

$$J_{ij} = \frac{\partial f_i}{\partial p_j} = \begin{cases} \sum_k \Gamma_{ik} + p_k(\Gamma_{ki} - \Gamma_{ik}) & i = j \\ -\Gamma_{ji} + p_i(\Gamma_{ji} - \Gamma_{ij}) & i \neq j \end{cases}. \tag{3.13}$$

As the initial value of $\boldsymbol{p}$ I have used a Fermi–Dirac distribution, with the temperature T given by the temperature of the system, and the chemical potential μ_c chosen to give the correct electron density.

3.5 Solving the balance equations with Newton's method

Before using Newton's method for solving the balance equations, a few practical issues need to be considered. Solving Eq. (3.11) demands a lot of memory, since $\boldsymbol{J}$ has N^2 elements, where N is the number of sites. Secondly, the equations (3.12) are not independent of each other. The equations have many solutions, corresponding to different total number of electrons. Finally, Newton's method is not guaranteed to converge to a solution, if the starting point is too distant from it. These three problems will be addressed below.

To decrease the memory demands of this method, one can treat $\boldsymbol{J}$ as a sparse matrix, as was done above in the linear, low-concentration case. Again, the hopping rates are set to 0 for all jumps longer than some cut-off length r_{cut}. Aiming at writing the whole solution algorithm as a GNU Octave or Matlab script, it is convenient to express equations (3.12) and (3.13) in matrix form, using the matrix $\boldsymbol{M}$ defined in Eq. (3.4).

$$\boldsymbol{f}(\boldsymbol{p}) = -\boldsymbol{M}\boldsymbol{p} + \text{Diag}(\boldsymbol{p})\ (\boldsymbol{M} - \boldsymbol{M}^T)\boldsymbol{p} \tag{3.14}$$

$$\boldsymbol{J}(\boldsymbol{p}) = -\boldsymbol{M} + \text{Diag}(\boldsymbol{p})\ (\boldsymbol{M} - \boldsymbol{M}^T) + \text{Diag}\left[(\boldsymbol{M} - \boldsymbol{M}^T)\boldsymbol{p}\right]. \tag{3.15}$$

Here, $\text{Diag}(\boldsymbol{p})$ is a diagonal matrix with the elements of the vector $\boldsymbol{p}$ on the diagonal.

As with the linear balance equations (3.1), the equations (3.12) are not independent. We again replace the first equation with

$$f_1(\boldsymbol{p}) \equiv \sum_i p_i - n = 0, \tag{3.16}$$

where n is the total number of electrons present. In this form the equations are independent, and there is (in general) a unique solution. The Jacobian is also modified, so that its first row consists of ones, $J_{1j} = 1$.

Newton's method does not necessarily converge if the starting point is too far from a solution. In the case of the balance equations, this turned out to be a problem in practice, especially at lower temperatures. The behavior can be improved by requiring that each step $\delta\boldsymbol{p}$ decreases $|\boldsymbol{f}|^2 = \boldsymbol{f}^T\boldsymbol{f}$ [51]. Unless this is the case, one takes a shorter step in the same direction, by scaling $\delta\boldsymbol{p}$ with some constant. It can be shown that moving in the direction given by $\delta\boldsymbol{p}$ initially decreases $|\boldsymbol{f}(\boldsymbol{p})|$, i.e. that $\delta\boldsymbol{p}$ gives a descent direction for $|\boldsymbol{f}|$. I implemented this by repeatedly dividing $\delta\boldsymbol{p}$ by 2, until $|\boldsymbol{f}(\boldsymbol{p} + \delta\boldsymbol{p})| < |\boldsymbol{f}(\boldsymbol{p})|$. This method, called the damped Newton method in Ref. 59, appears to work well, and improve the convergence when the starting point is chosen far from the solution. I also found it necessary to constrain the p_i:s to the interval $[0, 1]$ during the iterative procedure, by simply setting p_i to 0 or 1 whenever $p_i < 0$ or $p_i > 1$ respectively.

With the three additions mentioned above, Newton's method works well for solving the non-linear balance equations. It is numerically more robust, faster, and gives a more accurate result than the iterative method described above (at least when comparing my own implementations of the two methods), and has the advantage that the electron concentration is automatically correct, so that the rescaling procedure is not necessary. The price for these advantages is a larger memory demand. A way of further increasing the efficiency is to use the simplified Newton's method [59], where at each step one uses the Jacobian calculated for the first point, $\boldsymbol{J}(\boldsymbol{p}_0)$. Once $\boldsymbol{J}(\boldsymbol{p}_0)$ is calculated and $\boldsymbol{LU}$-factorized, solving the linear equation system in Eq. (3.11) can be done very efficiently for each new right-hand side. Even if a significantly larger number of iterations are needed for convergence in this scheme, it appears that the simplified method is faster than the regular Newton's method. One could of course determine the Jacobian at some points during the calculation, but it is not yet clear when it should be done.

The biggest remaining problem with Newton's method is the large amount of memory required for solving Eq. (3.11). The straight-forward solution method is to $\boldsymbol{LU}$-factorize $\boldsymbol{J}$. Even if $\boldsymbol{J}$ is sparse, the factors $\boldsymbol{L}$ and $\boldsymbol{U}$ need not be particularly sparse. The number of non-zero elements in $\boldsymbol{L}$ and $\boldsymbol{U}$ can be reduced by a well-chosen permutation of the rows and columns of $\boldsymbol{J}$. Apparently this is easier for a two-dimensional system than for a three-dimensional one, since a two-dimensional system can be solved with significantly less memory. The linear equation system Eq. (3.11) can also be solved with iterative methods, such as the biconjugate gradient method [51]. This approach saves memory at the cost

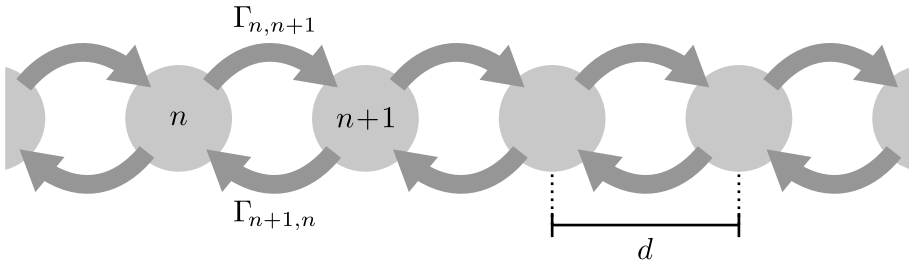

FIGURE 3.1 A one-dimensional chain of sites.

of added complexity, as one must make sure that the iterative linear method converges sufficiently at each iteration of Newton's method.

3.6 Derrida's expressions for transport in one-dimensional systems

For the special case of one-dimensional systems, there are methods more efficient than the general Monte Carlo and balance equation methods presented above. For nearest-neighbor hopping in a one-dimensional chain of sites, Derrida [60] derived expressions for the electron drift velocity v and diffusion coefficient D. In this section, Derrida's equations are given, without any derivation, together with a fast method for evaluating the expressions. We used this approach for studying diffusion in one-dimensional systems, as described in Chapter 6.

Derrida's expressions for v and D are given as functions of all the hopping rates Γ_{ij} in the chain, see Fig. 3.1. The chain is assumed to be periodic with the period N. Derrida derived the equations starting from the master equation,

$$\frac{dp_n}{dt} = p_{n+1}\Gamma_{n+1,n} + p_{n-1}\Gamma_{n-1,n} - p_n(\Gamma_{n,n+1} + \Gamma_{n,n-1}). \tag{3.17}$$

which describes how the occupation probabilities in the chain change in time. As this master equation is linear, the resulting expressions are valid in the limit of low electron concentration. The average velocity and diffusion constant are

given by

$$v = \frac{N}{\sum_{n=1}^{N} r_n} \left[1 - \prod_{n=1}^{N} \left(\frac{\Gamma_{n+1,n}}{\Gamma_{n,n+1}} \right) \right], \tag{3.18}$$

$$D = \frac{1}{\left(\sum_{n=1}^{N} r_n \right)^2} \left(v \sum_{n=1}^{N} u_n \sum_{i=1}^{N} i r_{n+i} + N \sum_{n=1}^{N} \Gamma_{n,n+1}\, u_n r_n \right) - v \frac{N+2}{2}, \tag{3.19}$$

where r_n and u_n are defined as

$$r_n = \frac{1}{\Gamma_{n,n+1}} \left[1 + \sum_{i=1}^{N-1} \prod_{j=1}^{i} \left(\frac{\Gamma_{n+j,n+j-1}}{\Gamma_{n+j,n+j+1}} \right) \right], \tag{3.20}$$

$$u_n = \frac{1}{\Gamma_{n,n+1}} \left[1 + \sum_{i=1}^{N-1} \prod_{j=1}^{i} \left(\frac{\Gamma_{n-j+1,n-j}}{\Gamma_{n-j,n-j+1}} \right) \right]. \tag{3.21}$$

Evaluating the equations as stated above takes time proportional to N^2 (the sum of products in Eq. (3.20) and (3.21) can be evaluated in N steps, since the product simply grows by one factor for each new term of the sum). By rearranging the calculations the result can be obtained in time proportional to N. This rearrangement will be presented below, since it is makes it practical to evaluate the expressions for chains with several million sites. In the following, we will assume that the field is directed so that the average electron drift is to the right, i.e. towards larger site indices. Define

$$g_n = \frac{\Gamma_{n,n-1}}{\Gamma_{n,n+1}}, \tag{3.22}$$

$$h_n = \frac{\Gamma_{n+1,n}}{\Gamma_{n,n+1}}, \tag{3.23}$$

$$G_n = 1 + \sum_{i=1}^{N-1} \prod_{j=1}^{i} g_{n+j} \tag{3.24}$$

$$H_n = 1 + \sum_{i=1}^{N-1} \prod_{j=1}^{i} h_{n-j}, \tag{3.25}$$

so that $r_n = G_n \,/\, \Gamma_{n,n+1}$ and $u_n = H_n \,/\, \Gamma_{n,n+1}$. All G_n and H_n, and thus r_n and u_n can now be calculated efficiently from the recurrence relations

$$G_{n-1} = g_n G_n - G + 1, \tag{3.26}$$

$$H_{n+1} = h_n H_n - H + 1 \tag{3.27}$$

where $G = H = g_1 g_2 \ldots g_N = h_1 h_2 \ldots h_N$. For the first term in the brackets in Eq. (3.19), define

$$S_n = \sum_{i=1}^{N} i r_{n+i} \qquad \text{and } S = \sum_{i=1}^{N} r_n. \tag{3.28}$$

Then the S_n obey the recurrence relation

$$S_{n+1} = S_n - S + N r_{n+1}. \tag{3.29}$$

As starting points for the three recurrence relations above, G_1, H_N, and S_1 should be calculated using Eqs. (3.24), (3.25), and (3.28). These relations are numerically stable if $G < 1$, which is satisfied if the average drift is to the right.

The drift velocity and diffusion coefficient are now given by

$$v = \frac{N}{S}(1 - H) \tag{3.30}$$

$$D = \frac{1}{S^2}\left(v \sum_{n=1}^{N} \frac{H_n S_n}{\Gamma_{n,n+1}} + N \sum_{n=1}^{N} \frac{G_n H_n}{\Gamma_{n,n+1}} \right) - v\frac{N+2}{2}. \tag{3.31}$$

It seems tempting to write Eq. (3.26) in the form

$$G_n = (G_{n-1} + G - 1)/g_n, \tag{3.32}$$

so that the sums in Eq. (3.31) could be evaluated from $n = 1$ without storing all G_n, but this form is too susceptible to numerical errors to be usable in practice. The problem with Eq. (3.32) is that $g_n < 1$ in average, and the repeated division by this quantity tends to amplify rounding errors. Thus one has to evaluate all G_n with Eq. (3.26) starting from $n = N$ and store them in a table. S_n and H_n do not need to be stored, since they can be evaluated while performing the sum in

Eq. (3.31), starting from $n = 1$. The equations (3.26) and (3.27) are numerically stable (for drift to the right), since the multiplication with the small quantities g_n and h_n tend to attenuate rounding errors instead of amplifying them.

This approach to calculate the transport properties of chains was used in Paper IV, where chains of up to 100 million sites were studied. There we also derived analytical expressions for the same quantities, for the particular case a Gaussian density of states, and a few different choices for the hopping rates. In the analytical approach, we no longer consider a particular chain with given hopping rates, we instead obtain the expected values of v and D from assumptions about the hopping rate and the distribution of site energies.

3.7 Comparing numerical methods

Now the main numerical methods of this work have been presented, the Monte Carlo method in Chapter 2 and the balance equation method in this chapter. I conclude the presentation of methods by a few notes on how the methods compare with each other and on how I have chosen which method to use in the different studies. The choice of method is influenced by many factors, for example the number of sites in the system, the cut-off length r_{cut} and whether or not interaction effects are important.

In the low-concentration limit the choice is quite simple, since the linear balance equation corresponds exactly to the one-particle Monte Carlo method. Since the balance equation method guarantees a steady state solution, and finds it efficiently, I would prefer it over the Monte Carlo method whenever the matrix equation can be solved in the amount of RAM memory available. Additionally, the balance equations directly give the occupation probability for each site. For these reasons, the balance equation method was used in Papers I and II.

When larger systems are needed, the Monte Carlo approach remains as the only option. In particular, Monte Carlo simulation on a lattice of sites is efficient in memory use. In the studies of diffusion in two- and three-dimensional systems, Paper V, very large systems were used, and for this application the lattice Monte Carlo method seemed to be the best choice. In the analogous study of diffusion in one dimension, we could apply the much more efficient methods that are special for the one-dimensional case.

For finite electron concentrations the situation is more complicated. Since the non-linear balance equations are derived under the mean-field approximation, they neglect all correlations between the occupancies of different sites. The Monte Carlo method, on the other hand, is exact in the limit of simulating an

infinite number of hops, in the sense that all correlations in site occupation are taken into account. Solving the balance equations seems faster than performing Monte Carlo simulations, but demand considerably more memory, as in the linear, single-particle case. The effects of the correlations were studied in Ref. 56, with the conclusion that the mean-field method is valid for practically interesting parameters. A small-scale comparison of results from a Monte Carlo simulation and the solution to the balance equations for the same system was made in Paper III. A good agreement between the two methods was found, but since a very small set of values for the different parameters were explored, this study does not permit general conclusions.

Chapter 4

Effective temperature for hopping transport

In studying charge transport in a material, we are interested in finding the electron flow in response to an electric field F. This flow is known to depend on the temperature T of the material. We are always interested in making the model as simple as possible. Therefore, we investigate if it is possible to express the combined effect of the temperature and the electric field using some combination of T and F. Such a combination of temperature and electric field is called the effective temperature, $T_{\text{eff}}(T, F)$.

In searching for the effective temperature, we will study the energy distribution of the electrons. The energy distribution is sensitive to both the temperature and to the electric field. Furthermore, both a high electric field and a high temperature qualitatively influence the distribution in the same way, both of them enable the electrons to visit sites with higher energies. In fact, it turns out that the effect on the energy distribution of applying an electric field can be approximated by the effect of increasing the temperature. For this reason the effective temperature concept seems promising. Once an effective temperature has been determined from the electron energy distributions, we will return to studying electron flow, by trying to express the electron mobility μ as a function of the effective temperature.

The effective temperature concept was first developed and tested for the case of an exponential density of states [38, 57, 61, 62]. In Paper I we show that the concept is applicable also for a Gaussian density of states, and that the electron mobility, in particular its field dependence, can be expressed using the effective temperature. This conclusion is important, since it allows the application of the

effective temperature concept for organic materials, where the density of states is believed to be Gaussian. Also, since the mobility's field dependence is not easily expressed while its temperature dependence is known, it may be a useful approximation to express the mobility as a function of the effective temperature.

In Section 4.1 the energy distribution of electrons is given for the case without an electric field. The electrons follow a Fermi–Dirac distribution in this case. Section 4.2 describes the more complex situation with an electric field. The effective temperature is introduced for describing the energy distribution. In Section 4.3 the result of Paper I is presented, namely that the effective temperature is applicable for systems with a Gaussian distribution of site energies. Conclusions and a few references to other recent publications on the same topic are gathered in Section 4.4.

4.1 Energy distribution of electrons at zero field

We will determine the effective temperature using the energy distribution of the electrons. The quantity that will be most useful to us is the site occupation probability as a function of site energy, $p(\varepsilon)$. Let us first discuss the situation without an electric field.

Consider a single electron hopping in an otherwise empty system of sites, with the hopping rate (1.3). The occupation probability p_i for site i is simply given by the Boltzmann distribution

$$p_i = p(\varepsilon_i) \propto \exp(-\varepsilon_i/kT). \tag{4.1}$$

If one assumes this distribution, one can see that the net electron flow between any pair of sites is zero. Thus the p_i:s satisfy the linear balance equation (3.3), meaning that Eq. (4.1) gives the occupation probabilities for the steady state. This is equivalent to stating that the Miller–Abrahams hopping rate obeys the condition of detailed balance,

$$\frac{\Gamma_{ij}}{\Gamma_{ji}} = \exp\left(\frac{\varepsilon_i - \varepsilon_j}{kT}\right), \tag{4.2}$$

something that can be expected of any reasonable model for the hopping rate.

The steady state energy distribution ρ_e of the electrons can now be expressed as

$$\rho_e(\varepsilon) = p(\varepsilon)g(\varepsilon), \tag{4.3}$$

where $g(\varepsilon)$ is the density of states. For the Gaussian density of states of Eq. (1.8) one finds that $\rho_e(\varepsilon)$ is a Gaussian function of width σ centered at the average electron energy $\langle\varepsilon\rangle = -\sigma^2/kT$ [9, 13, 25].

If one instead considers several electrons, and solves the non-linear balance equation (3.1) for the case of no electric field, one obtains the Fermi–Dirac distribution

$$p_i = p(\varepsilon_i) = \frac{1}{1 + \exp\left[(\varepsilon_i - \mu_c)/kT\right]}. \tag{4.4}$$

Here μ_c is the chemical potential, determined by the number of electrons in the system.

4.2 Energy distribution at non-zero field

We now turn to the energy distribution of the electrons in the presence of an electric field F. Since we are interested in a system where a current flow is possible, we consider either an infinite system or a finite system with periodic boundary conditions. The considerations of the previous section no longer applies with a finite electric field. Since the electric field causes a net current to flow, one can no longer obtain the occupation probabilities of the sites by just considering the flow balance between two sites at a time. A way to proceed is to numerically solve the occupation probabilities for all sites, and to determine the occupation probability $p(\varepsilon)$ as a function of site energy ε. Some variant of the balance equation method (Chapter 3) is suitable, since it directly gives the occupation probabilities for all sites in the system.

In the presence of an electric field, the electrons tend to occupy states of higher energy than in the case without an electric field. Interestingly, when an electric field is applied, $p(\varepsilon)$ almost retains its Fermi–Dirac shape, but with the temperature replaced by some higher value. To describe the shape of the energy distribution at non-zero field, the effective temperature T_{eff} is introduced. The effective temperature $T_{\text{eff}}(T, F)$ is the temperature parameter that best describes site occupation probabilities, when the temperature is T and the electric field is F. The effective temperature defined in this way can be determined numerically, by solving the occupation probabilities p_i in a system for given F and T, and then fitting $p(\varepsilon)$ with the Fermi–Dirac function (4.4).

The idea that the electric field plays a similar role as the temperature for the transport process was first suggested by Shklovskii [61]. A high temperature gives the electron access to sites with a high energy, whereas a large electric field gives the electron access to high energy sites in the transport direction.

For the case of an exponential density of states Eq. (1.7), Marianer and Shklovskii [57] verified the idea by numerical simulations, and obtained an expression for the effective temperature

$$T_{\text{eff}} = \left[T^{\beta} + \left(\gamma \frac{eFa}{k} \right)^{\beta} \right]^{1/\beta}, \tag{4.5}$$

with $\beta = 2$ and $\gamma = 0.67$. The effective temperature was determined by solving a system of linear balance equations (see Section 3.1) for the site occupation probabilities in a randomly generated system, and then fitting the occupation probabilities with the Boltzmann function (4.1). It was also found that the conductivity could be expressed as a function of the same effective temperature.

Later it was shown with many particle Monte Carlo simulations [38] that the relaxation time of the electrons and the electron energy distribution both can be given as functions of T_{eff}. The values obtained for $T_{\text{eff}}(T, F)$ were found to agree with the result of Marianer and Shklovskii (4.5). Further Monte Carlo studies [62] showed, however, that the steady state electron mobility can not be given as a function of the effective temperature given above. The mobility could instead be described as a function of a different effective temperature, with $\gamma = 0.89$ in Eq. (4.5). This seems to disagree with Marianer and Shklovskii's result for the conductivity. A reason for the different conductivity results might be that Marianer and Shklovskii calculated in the limit of low electron concentrations (since they solved linear balance equations), while the Monte Carlo simulation had a finite electron concentration.

4.3 Effective temperature for a Gaussian energy distribution

All the studies discussed above were performed for the case of an exponential density of states. Is the concept of effective temperature also applicable in the case of a Gaussian density of states? In Paper I it is shown that the effective temperature is a useful concept also for a system with a Gaussian energy distribution. Both the electron energy distribution and mobility are shown to be described by an effective temperature given by Eq. (4.5) with $\beta = 1.54 \pm 0.2$ and $\gamma = 0.64 \pm 0.2$. The simulations in Paper I were performed with the method of non-linear balance equations described in Chapter 3. Simulation results for the occupation probability p as a function of site energy ε are shown in Fig. 4.1a for different electric fields. As the electric field is increased the electron distribution

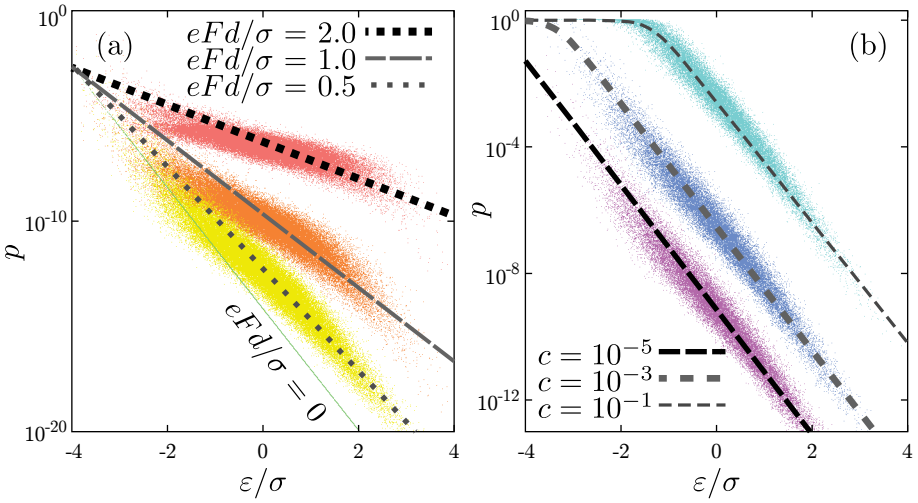

FIGURE 4.1 Occupation probability p as a function of site energy ε. (a) results for different electric fields F in the limit of low electron concentration. Note that the point cloud for $F = 0$ lies exactly on a line, since the occupation probability for this case is exactly given by the Boltzmann distribution. The system contains 40^3 sites, and the parameters are $kT = 0.15\sigma$ and $a = 0.3d$. (b) A similar plot for different electron concentrations c. The curves show fitted Fermi–Dirac functions. The results were obtained by solving the non-linear balance equations using Newton's method (Section 3.4). The system contains 30^3 sites. The parameters are $kT = 0.2\sigma$, $eFd = 0.4\sigma$, and $a = 0.3d$.

remains Boltzmann-shaped, but the slope becomes less steep, indicating a rise in the effective temperature. With the non-linear balance equations, the concentration of electrons in the system can be varied. Interestingly, it turns out that the effective temperature determined by fitting the occupation probabilities is independent of the electron concentration. When the electron concentration is changed only the chemical potential μ_c is affected. An example of this behavior is shown in Fig. 4.1b. Here $p(\varepsilon)$ is shown for different electron concentrations. The slopes of the the different curves are equal, showing that the effective temperature is independent of the electron concentration. Figure 4.1 also shows that there is a considerable spread in occupation probabilities for sites with almost the same energy, except in the zero-field case where $p(\varepsilon)$ is exactly the Fermi distribution. This means that when an electric field is applied, the probability for a given site to be occupied is not completely determined by its energy, but also influenced by the configuration of other sites in the environment.

The effect of introducing correlations [16–19] between the energies of spatially close sites is also investigated in Paper I. In the case of a correlated disorder, an effective temperature that is independent of the electron concentration can still be determined. The effective temperature increases with an increasing correlation length, and is thus no longer given by Eq. (4.5). Also the mobility in general increases with increasing correlation length (except in the case of randomly placed sites, but this is due to the way in which the correlations were introduced). Thus the electric field has stronger effects when correlations smoothen the potential landscape.

4.4 Further studies and conclusions

The effective temperature was introduced in the hopping transport picture as a way of describing the energy distribution of the electrons. The concept was introduced [61] and numerically verified [38, 57] for systems with an exponential density of states. In Paper I it was shown that the effective temperature concept can also be applied in a system where the density of states is Gaussian, suggesting that the idea is usable for organic semiconductors. The field dependence of the electron mobility was expressed through the effective temperature. It was also shown that the effective temperature is independent on the electron concentration and that the idea remains useful when correlations are introduced between the energies of spatially close sites.

The relationship between mobility and the effective temperature has been investigated experimentally. Mobility data, measured in RR-P3HT for varying

electric field and temperature was analyzed using the effective temperature [1]. An effective temperature $T_{\text{eff}}(T, F)$ with the shape of Eq. (4.5) could be determined, so that the mobility $\mu(T_{\text{eff}})$ for all temperatures and fields collapsed onto a single curve, meaning that the mobility in this case could be expressed as a function of an effective temperature.

The results obtained in Paper I have recently been tested by Vukmirović and Wang, in a detailed multi-scale simulation study of one particular semiconducting polymer, P3HT [63]. The structure of the material was obtained by a molecular dynamics simulation. Using that structure, the electronic states were found using density functional theory, and the transition rates from one state to another were found by Fermi's golden rule. In this system, it was found that the energy distribution of the charge carriers could be described by an effective temperature. The carrier mobility however, could not be expressed as a function of this effective temperature. The authors explained this to be a consequence of the choice of hopping rates. When using Miller–Abrahams hopping rates instead of the more complicated ones given by their model, their mobility values were much better described as a function of the effective temperature. Regarding the multi-scale approach, it should be noted that it seems to introduce a correlation between the energies of spatially close sites (sites within the same "small box", in step 5 of the method in Ref. 63). As described above, such a correlation may affect both the carrier mobility and the effective temperature determined from the carrier energy distribution.

Tutiš, Jurić and Batistić investigated the applicability of the effective temperature idea in one dimension [64], obtaining the site occupations with a method based on that of Derrida [60]. In this way both analytical and numerical results were obtained. In the low-field limit, the effective temperature was found to be of the form of Eq. (4.5), with the parameters

$$\beta = 1 \qquad \text{and } \gamma = \frac{1}{2}\exp\left(-\frac{\sigma^2}{2(kT)^2}\right). \tag{4.6}$$

The same authors repeated and extended [65] the study of effective temperature with a Gaussian density of states described in this chapter. They confirmed that the site occupation probability $p(\varepsilon)$ approximately retains its Fermi–Dirac shape at non-zero fields, but did not find a good agreement with Eq. (4.5), perhaps due to the wider ranges of parameters used.

Finally it should be noted that describing the electron mobility and energy distribution as functions of an effective temperature should be considered as approximations. From the spread in occupation probability for sites with nearly equal energy one can see that the effective temperature is not sufficient for an

exact description of the hopping process at non-zero fields. This dependence of the occupation probability of a site on the environment was also noted in the one-dimensional study cited above.

Chapter 5

Negative differential conductivity

There are electrical components that behave in such a way, that when the voltage applied over the device is increased, the current through the device drops. This phenomenon is called negative differential conductivity (NDC). The current-voltage curve for such a component is illustrated in Fig. 5.1a. Esaki's tunnel diode [66] and the Gunn diode behave in this way. With a resistor and a component showing NDC one can construct a circuit with two stable states, which can then be used as a one-bit memory. This chapter deals with negative differential conductivity in the hopping transport model. The research was inspired by measurements on organic memory devices.

Large efforts have been made to develop memory devices made from organic materials. These devices typically consist of a layer of conductive particles embedded in a nonconductive medium between a pair of contacts, as shown in Fig. 5.1b. Such devices have been made from both inorganic [67, 68] and organic [3, 69–75] materials. Measurements on these devices often show an NDC effect. The devices also typically show memory effects, in the sense that the current through the device may depend not only on the applied voltage but also on the history of what voltages have been applied previously. The mechanism of these devices is not well understood. Since the hopping transport model seems to be a reasonable starting point to model these memories (or at least some aspects of them), it is interesting to look for mechanisms leading to NDC within the hopping transport model. This is the aim of the present chapter and of papers II and III.

Two completely different mechanisms that can lead to NDC in the hopping transport model will be described, together with results of computer simulations where the mechanisms are seen. Section 5.1 describes how NDC can arise due

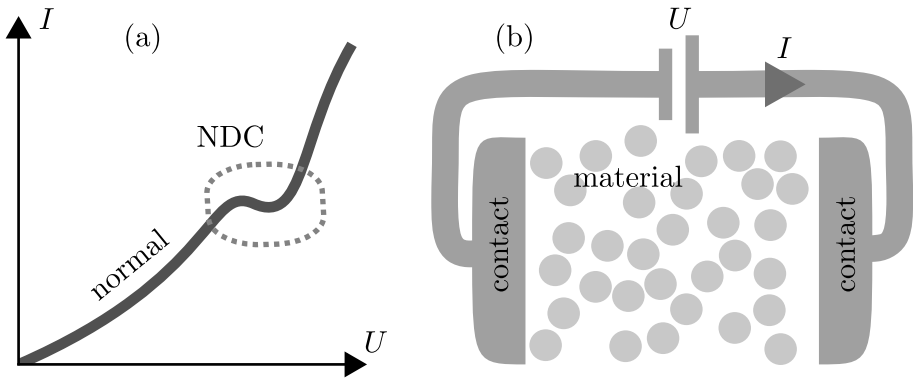

FIGURE 5.1 (a) Current-voltage curve illustrating negative differential conductivity. (b) The structure of the memory device.

to the trapping of electrons in dead ends, that is on sites that are hard to leave when the electric field is large. Section 5.5 shows that NDC can arise also due to the Coulomb interaction between electrons in the material, the Coulomb blockade effect.

5.1 Trapping and negative differential conductivity

Nguyen and Shklovskii [76] predicted that negative differential conductivity (NDC) can arise in the hopping transport model at high electric fields via a trapping mechanism. The aim of the work presented in Paper II was to test this prediction by numerical simulations. The simulation and the numerical results are described below, but let us start with the model of Nguyen and Shklovskii.

The central idea in the theory is that at high electric fields the transport of an electron will be determined by sites that are hard to escape due to the high electric field. These sites are those that have no close neighbors in the transport direction, so that to leave one of them the electron either has to make a long jump in the transport direction or return against the field. In a high field both of these processes are slow. We will call this kind of site a trap. In discussing hopping transport the word trap is often used to describe a site that is hard to escape due to its low energy. Here, however, the trap is hard to escape for geometrical reasons, the distribution in space of the neighboring sites. Furthermore, escaping the trap in the direction against the transport direction

is more difficult when the field is large. Thus the time an electron spends in a given trap increases with an increasing electric field. This is the reason for the NDC in the theory. We will now derive an expression for the electron drift velocity as a function of the electric field by considering the contributions from traps of different size and shape.

Assume the sites are randomly distributed in three dimensions, with the concentration N. Also assume that the electric field is large, so that the energetic disorder of the sites can be ignored, simplifying the analytical treatment. (We will consider the effects of energetic disorder below, in the discussion of computer simulations where the energetic disorder can easily be taken into account.) In this picture the electron transport will be controlled by the electric field and the distribution of sites in space. In the limit of an infinite electric field, the electrons can hop only in the direction against the field. If the field is large but finite, jumps against the field are possible but difficult.

Consider a site with no close neighbors on its right hand side, as shown in Fig. 5.2a. The field is directed so that it pulls the electrons to the right, along the x axis. In the limit of infinite field, the electron can escape this site only by a long slow hop to the right. This site will act as a trap for the electrons in the limit of an infinite field. At finite fields, the electron can also escape the site by hopping to the left, thus the trapping time will be shorter for smaller fields. At finite fields traps with a different shape are more efficient, such as the one shown in Fig. 5.2b, where the cone-shaped part makes it more difficult to escape by returning to the left.

To obtain expressions for the electron drift velocity, we consider first the limit of an infinite electric field and then the case of a large but finite field. This treatment follows the path of Nguyen and Shklovskii and the derivations in Paper II. Here, only the limit of a small electron concentration will be considered. The case of finite electron concentration is treated in Paper II and in Ref. 76.

5.2 Trapping at infinite field

At each jump the electron moves a distance approximately R in the x direction, where $R = N^{-1/3}$ is the typical distance between neighboring sites. By defining $\overline{\tau}$ as the average dwell time on a site, the electron drift velocity v can be estimated as $v \simeq R/\overline{\tau}$. According to Eq. (1.3) the dwell time on site i is proportional to $\exp(2r_i/a)$, where r_i is the distance from site i to its closest neighbor to the right of i. The contribution of traps with radii in the range $[r, r + dr]$ to the average dwell time $\overline{\tau}$ is proportional to $\tau(r) = \exp(2r/a)$, and also to the probability for

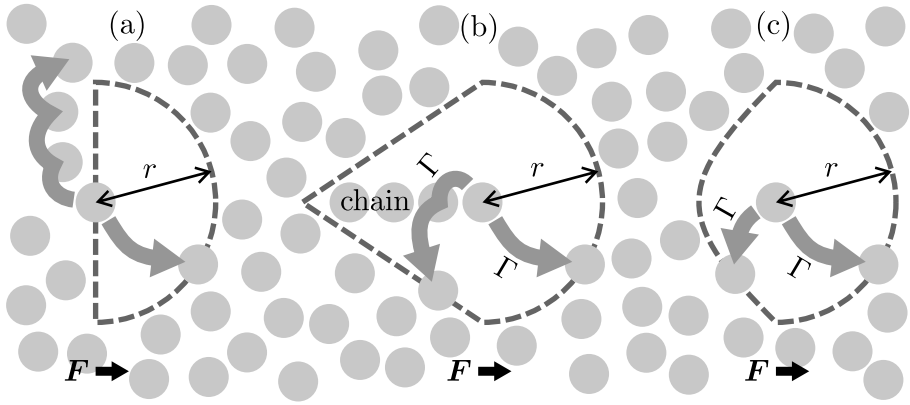

FIGURE 5.2 Different trap shapes. (a) A site without close neighbors in the transport direction acts as a trap at infinite field. At smaller fields, the path to the left provides a faster way to leave the trap. (b) An effective trap at finite fields. The chain of sites provides a path into the trap. The shape is defined so that it is equally hard to escape the trap to any point on its surface. (c) Another trap at finite field, without the chain.

a given site to have its nearest right-hand neighbor at a distance between r and $r + dr$: $p(r)dr = 2\pi N r^2 \exp(-2\pi N r^3/3)dr$.

$$\overline{\tau} = \int_0^\infty \tau(r)p(r)dr = \int_0^\infty 2\pi N r^2 \exp\left(\frac{2r}{a} - \frac{2\pi N}{3} r^3\right) dr. \tag{5.1}$$

The integrand has a sharp maximum at $r = r_m = 1/\sqrt{\pi N a}$. Thus the traps with radius r_m contribute the most to $\overline{\tau}$. Nguyen and Shklovskii call these most important traps optimal. Using the sharp maximum of the integrand the integral can be approximated. We obtain an expression for the current density

$$j_{F\to\infty} \simeq \frac{n_e R}{\overline{\tau}} \simeq n_e (a^3 R)^{1/4} \exp\left(-\frac{4}{3\sqrt{\pi}} \left(\frac{R}{a}\right)^{3/2}\right), \tag{5.2}$$

where n_e is the electron concentration, in the large-field limit.

5.3 Trapping at finite field

At a finite field, a hemispherical trap shape is not the most efficient one, since the electrons can escape the trap also by moving back along the field. This is illustrated by the left arrow in Fig. 5.2a. In this case Nguyen and Shklovskii proposed that the optimal traps have the shape illustrated in Fig. 5.2b, with a hemispherical part with radius r to the right and a cone with height h to the left. A chain of sites along the x axis provide an easy path into the trap. The height h of the cone is chosen so that it is equally hard to escape the trap in any direction, taking the chain of sites into account, or stated differently, the hopping rate to any point on the trap's surface is the same.

$$h = 2rkT/Fa. \tag{5.3}$$

The volume of a trap of this shape is

$$V_{\text{trap}} = \left(1 + \frac{kT}{Fa}\right) \frac{2\pi r^3}{3}. \tag{5.4}$$

For this trap volume one obtains the current density as a function of the electric field as

$$j \simeq n_e (a^3 R)^{1/4} \exp\left[-\frac{4}{3\sqrt{\pi}} \left(\frac{R}{a}\right)^{3/2} \left(1 + \frac{kT}{Fa}\right)^{-1/2}\right]. \tag{5.5}$$

The current density given above decreases with an increasing field, and approaches the value given in Eq. (5.2) when $F \to \infty$. The expression is valid only when $F \gg kT/R$. For smaller fields, the assumption that almost every jump is directed along the axis x is violated. At low fields ($F \ll kT/R$) one would instead expect a region of Ohmic conductivity, $j \propto F$.

5.4 Simulation of the NDC effect

We performed computer simulations to test the predictions of the theory outlined above, and to study the transport at low and intermediate field. The calculations were performed on systems consisting of $N = 8000$ sites randomly distributed inside a cube with the side length $L = 20R$, with periodic boundary conditions in all directions. The electron drift velocity as a function of the electric field was determined with the linear balance equation method described in Section 3.1, see Fig. 5.3. Both the theoretical and the numerical results show

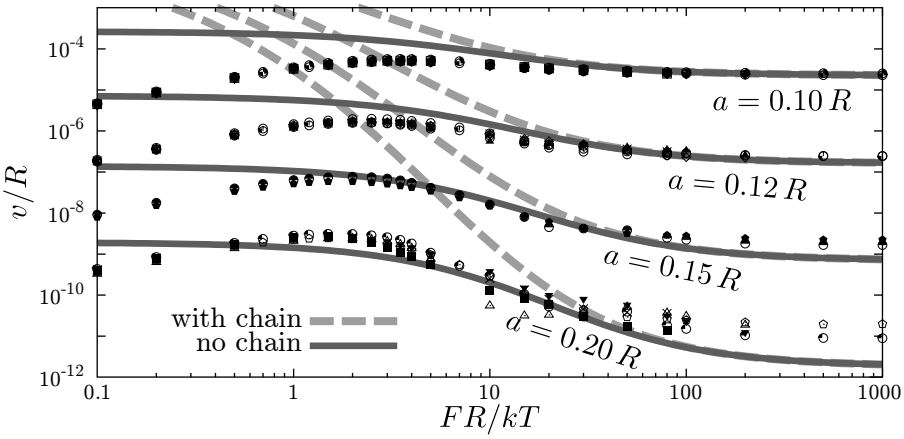

FIGURE 5.3 The electron velocity as a function of the electric field, for different localization lengths a. The symbols show simulation results, while the dashed curves show the expression of Nguyen and Shklovskii and the solid curve shows the result for traps without the chain.

that the NDC effect is more pronounced the more dilute the system is, i.e. the smaller the localization length a is in comparison to the typical nearest-neighbor distance R. The figure indicates that although the simulation results agree with the theory in the high-field limit, the theory predicts a much steeper field dependence (dashed curves) than the one seen in the simulations. This discrepancy is present also at such high fields ($F \gg kT/R$) that the theory should be applicable. This led us to try to change the assumption about the trap shape in the theory, by removing the chain of sites leading in to the trap (Fig. 5.2c). The result for traps without the chain leading in to them is shown in Fig. 5.3, with solid curves. As the field dependence predicted with this shape is much weaker than with the cone-shaped traps, the traps without chains give a closer fit to the simulation data.

Some information about the shape of the most important traps can also be extracted from the simulation data. Since the balance equation method gives the occupation probability of each site, it directly tells us on which sites the electron spends the most time. Fig. 5.4 shows the time averaged density of *neighbor sites* around the position of the electron. Sites where the electron spends much time will then contribute strongly to the displayed result. The figure supports the idea of hemispherical traps at high electric fields. The trap radius also corresponds

closely to the optimal trap radius r_m, see the comparison in Paper II. At lower fields on the other hand, neither the cone-shaped trap nor the trap without a chain seem to give a perfect description. Note that to the left of the trap is an area with a higher than average density of sites, which supports the idea of a chain leading into the trap.

In the simulation it is easy to study the effect of disorder in the site energies. The result is shown in Fig. 12 in Paper II. Increasing the magnitude of the disorder decreases the peak electron velocity. On the other hand at higher electric field the velocity is less affected by disorder. Thus the NDC effect gradually disappears when the energetic disorder is increased.

We have now seen how the random distribution of transport sites in space creates geometric traps for the electrons, and that the traps are more efficient at high fields. The predictions of Nguyen and Shklovskii were confirmed by computer simulations, but the field dependence of the electron velocity turned out to be weaker than theoretically predicted.

In the model considered above, the random distribution of sites in space was an essential feature. However, it is possible to obtain NDC also in lattice models. Gartstein, Jeyadev and Conwell simulated hopping transport at high fields on a lattice with bond percolation [77]. They observed the NDC effect, and attributed it to a trapping effect similar to the one described above, namely that the electrons are trapped in places where an "easy" escape route goes against the transport direction given by the field.

5.5 Coulomb blockade in the hopping transport model

A completely different mechanism leading to NDC in the hopping transport model was suggested by Shin et al. [78]. While the NDC in the previous section was caused by geometrical traps, the NDC in this model is caused by Coulomb interaction between the electrons, specifically by Coulomb blockade. Shin et al. considered a system with four sites placed between two contacts, as shown in Fig. 5.5. The contacts act as electron reservoirs at different potential. Electrons can hop from the contacts to sites in the system, as long as it is energetically favorable. At low electric fields, at most one electron at a time is present in the system. When the voltage is increased, the electron moves through the system faster, due to the increased electric field. This is seen as an increasing current. But when the voltage is increased to the point where a second electron can be injected into the system, the current suddenly drops. The reason for this behavior is that the two electrons tend to occupy the two middle sites. Neither

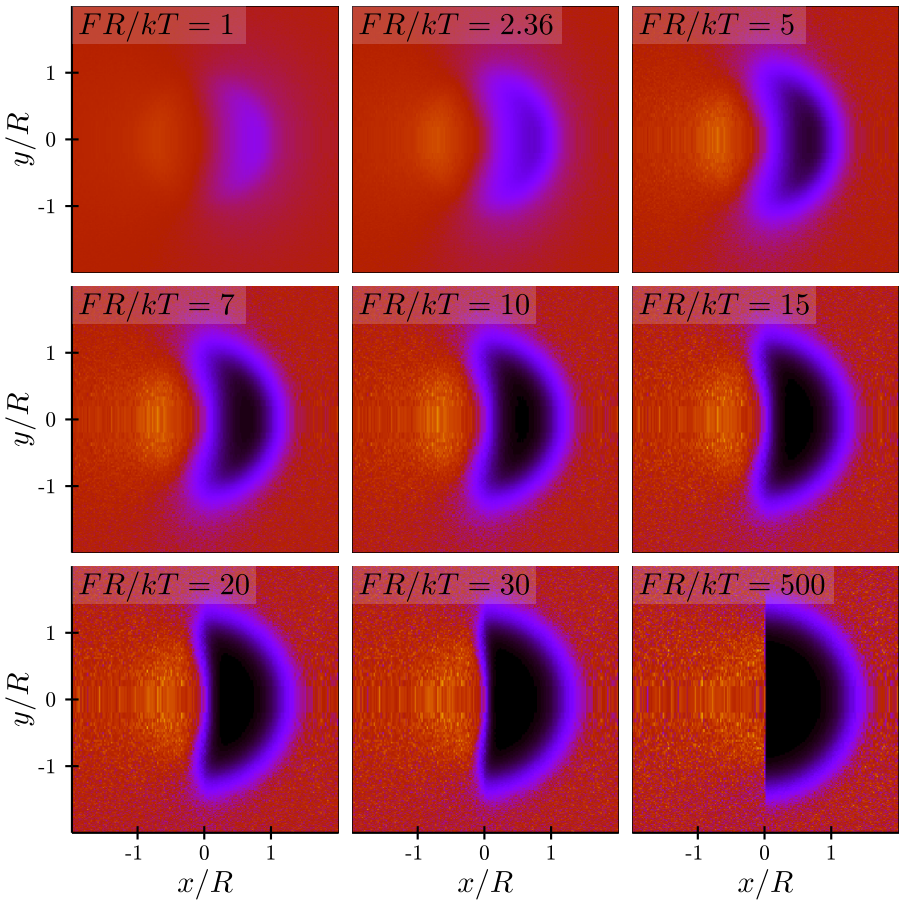

FIGURE 5.4 Time average of the density of sites around the position of the electron for different electric fields. When the field is increased, the shape of the trap approaches a hemisphere, as predicted. To the left of the trap an area with increased site concentration is seen, corresponding to the chain of sites leading to the trap.

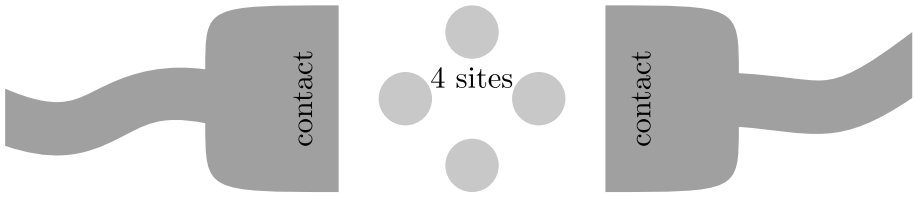

FIGURE 5.5 Four sites between a pair of contacts, the system of Ref. [78].

of the electrons can easily hop out of this configuration, since that would take it closer to the other electron, which would be energetically unfavorable. There is a voltage range where the two-electron configuration is stable and the current is small. Increasing the voltage beyond this range again leads to an increasing current. From this, we see how the NDC effect arises in this four-site system.

The aim of Paper III is to find out under which conditions the Coulomb blockade is possible, and whether or not the Coulomb blockade effect is to be expected in a larger, more general system for example one consisting of randomly placed sites. First of all, merely including the Coulomb interaction into the hopping transport model seems not to be enough for NDC to appear. Hopping transport with Coulomb interaction has been studied extensively in the context of the Coulomb glass [21, 37, 42, 43], and also regarding transport properties [39–41]. In these studies, with a fixed number of charge carriers in the simulated system, no NDC effects have been reported. Also in our own simulations described in Paper III we could not obtain the NDC effect with a fixed number of electrons hopping in an "infinite" system (a system with periodic boundary conditions).

An important feature of the model by Shin et al. is that the number of electrons present in the system is not fixed, but may vary as a function of time and the applied voltage. Electrons are injected from the contacts as long as it is energetically favorable, which makes the number of electrons present in the device depend on the voltage. In the four-site system, the current decreases precisely when the voltage is increased above the threshold for injecting a second electron.

Many configurations of sites with similar properties as the one suggested by Shin et al. can be constructed. One example is given in Fig. 5.6, together with a plot of the current and the number of electrons present as functions of the applied voltage. The current was calculated by many-particle Monte Carlo simulations, as described in Section 2.8

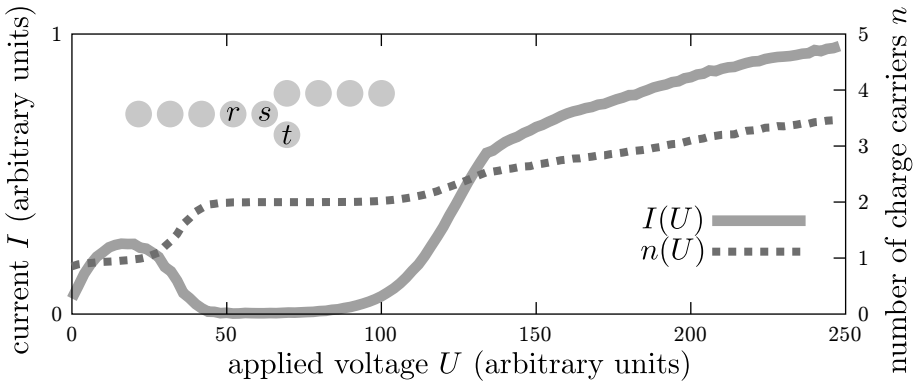

FIGURE 5.6 The current I as a function of the applied voltage U for the chain of sites shown in the inset. The average number of electrons in the chain, n, is shown by the dotted curve. The current minimum appears at the voltage where a second electron can enter the chain. The blocking configuration is the one where sites r and t are occupied. In that configuration, neither of the two electrons can easily hop to site s, since the presence of the other electron makes this jump energetically unfavorable.

We have now seen that if both contacts and the Coulomb interaction are included in the hopping transport model, Coulomb blockade effects can appear and be seen as regions of NDC in a current-voltage plot. Let us now turn to what is required of the site configuration in order for the NDC to appear. Does the Coulomb blockade appear when the sites are distributed randomly in space? The behavior of randomly generated systems is studied in Paper III. The systems consist of 125 sites between a pair of contacts. With suitably chosen parameters (localization length, disorder amplitude, and relative strength of the Coulomb interaction), regions of NDC reliably appear for different realizations of the system. However, since the systems are very small, there is a considerable variation from one realization to the next, and in some cases no NDC at all appears. It would be interesting to have results for systems that are so large that different realizations behave consistently.

5.6 Discussion

Finally a brief note about the applicability of the two NDC mechanisms described above to the memory devices. Both the geometrical traps and the Coulomb blockade can cause NDC, but there seems to be no simple way to obtain memory effects in the model of geometrical traps. In the Coulomb blockade picture, however, memory effects seem possible in principle. One could imagine, for instance, that the application of a voltage pulse (write) pushes the system into a stable, blocking configuration, where it would stay until a different pulse (erase) pushes the system out of this configuration and into another one, with a different conductivity. Between these pulses the state of the system could be read by applying a small voltage and measuring the current. The read voltage should be so small that it does not affect the system's state. This picture is reminiscent of the working principle of the flash and EEPROM (Electrically Erasable Programmable Read-Only Memory) memories.

Chapter 6

Diffusion in the hopping transport model

So far, we have considered how the electrons, on average, move in response to an applied electric field. But individual electrons do not just travel with the average velocity, they also move about randomly, diffuse. If one starts with a small packet of electrons, the packet will spread out as time passes due to electron diffusion. This chapter considers diffusion in the hopping transport model, particularly the drastic influence of an electric field on the rate of diffusion.

Although this chapter will be theoretical, diffusion in disordered materials also has a practical significance. The next chapter investigates one consequence of diffusion, namely the influence of diffusion on the recombination process, which is important in solar cell applications. Another application where diffusion is important is time-of-flight measurements. In time-of-flight experiments the diffusion of the charge carriers in a material can be measured. Furthermore, as described in Section 2.6, diffusion will always affect time-of-flight results, as the time needed for a charge carrier to cross a finite sample necessarily depends on both its drift and diffusive motion.

While the mobility could be defined in terms of the velocity of a single electron, the diffusion coefficient is defined for a packet of electrons,

$$D_x = \frac{\langle x^2 \rangle - \langle x \rangle^2}{2t}. \tag{6.1}$$

The diffusion coefficient measures how quickly the packet broadens (relative to

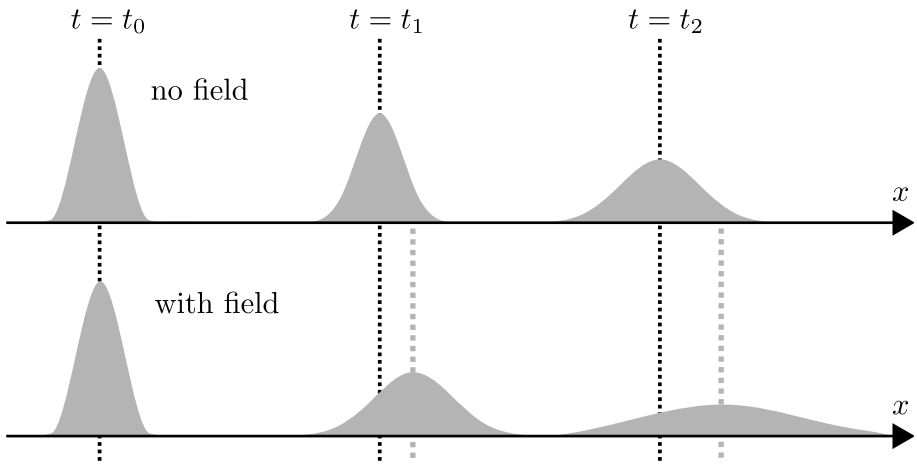

FIGURE 6.1 A packet of charge carriers broadens due to diffusion. In an electric field, the packet both broadens and drifts due to the field. Notably, the rate of broadening increases with increasing electric field.

its center), while the mobility measures the packet's average velocity:

$$\mu = \frac{\langle x \rangle}{Ft}. \tag{6.2}$$

In this chapter we study how the diffusion coefficient D depends on the temperature T and the electric field F, for electrons undergoing hopping transport. We will assume that the sites in the system have a Gaussian energy distribution (1.8), and that the Miller–Abrahams hopping rate (1.3) applies. In particular, we will see that the diffusion coefficient is strongly dependent on the strength of the electric field. The stronger the field is, the faster the electron packet broadens. This behavior is illustrated in Fig. 6.1, where the time-evolution of a packet of electrons is shown, both with and without an electric field.

In the limit of small electric field, the diffusion coefficient D and the mobility μ are related by the Einstein relation [79],

$$\mu kT = eD. \tag{6.3}$$

As the diffusion coefficient depends on the electric field, we have to ask if the relation is applicable for finite fields. The mobility μ also depends on the electric

field, but the dependence turns out to be much weaker than for the diffusion coefficient. Thus the Einstein relation (6.3) holds only in the small-field limit.

Paper IV describes diffusion in a one-dimensional system, while diffusion in two and three dimensions is studied in Paper V. This division was chosen, since the one-dimensional systems behave very differently from two- and three-dimensional systems. Additionally, both an analytical treatment and a special, efficient numerical method are possible in the one-dimensional case. Below I will summarize the results presented in the two articles, and discuss the methods used to obtain them. Section 6.2 describes diffusion in a one-dimensional system, while two- and three-dimensional systems are discussed in Section 6.3. The multiple trapping approximation, which was used to find out which sites are most decisive for determining the diffusion coefficient is discussed in Sections 6.4 and 6.5. Section 6.6 gives a brief note on the validity of Einstein's relation. First I will give some general observations on diffusion in the hopping transport model.

6.1 General results on diffusion

Regardless of the number of dimensions, the diffusion coefficient along the field's direction increases with the electric field, even at such small fields that the mobility still is independent of the field. The Einstein relation (6.3) is valid only in the low-field limit. In two and three dimensions, one can also calculate a diffusion coefficient perpendicular to the field. This perpendicular diffusion coefficient is much less sensitive to the field strength, and for it the Einstein relation remains a good approximation to much higher fields, see Fig. 6.5 below.

The strong field-dependence of the diffusion coefficient appears due to trapping of the electrons on rare sites with a very low energy. This statement is supported by the observations in Paper V on which sites are most important for determining the mobility and the diffusion coefficient: sites at the average electron energy $\langle\varepsilon\rangle = -\sigma^2/kT$ determine the mobility, while the much deeper sites around $\varepsilon^* = -2\sigma^2/kT$ determine the diffusion in the presence of an electric field. Qualitatively the field dependence of diffusion can be explained in the following way. Consider a packet of electrons, moving with some average velocity $\langle v\rangle$. If one of the electrons in the packet gets trapped for a long time on a low-energy site, the rest of the packet moves away from it. In this way, trapping contributes to the broadening of the electron packet, and the distribution of dwell times is converted into a distribution of electron positions.

In two and three dimensions, the diffusion coefficient depends quadratically

on the electric field, with an increasingly steep dependence for decreasing temperatures. In one dimension, the diffusion coefficient depends linearly on the field, for small fields. These observations have been reported previously. The quadratic field dependence in three dimensions was reported by Richert et al. [28]. The linear behavior in one dimension was reported by Bouchaud and Georges [80], albeit with a different model for the hopping rates. These surprisingly different behaviors reported for different number of dimensions is what prompted us to study diffusion in the hopping transport model. In particular, we wanted to find out whether the linear dependence reported in one dimension is a property of one-dimensional systems or if it appeared because of the different choice of the hopping rates. As reported in paper Paper IV, the linear dependence was observed in a one-dimensional system also with Miller–Abrahams hopping rates. Thus the linear behavior seems to be a robust property of one-dimensional systems, and to be insensitive to the details of the hopping rate. Let us now turn to the details of the diffusion process first in one dimension, and then in two- and three-dimensional systems.

6.2 Diffusion in one dimension

As described in Section 3.6, Derrida derived expressions for the mobility μ and the diffusion coefficient D for nearest neighbor hopping in a one-dimensional chain of sites, as functions of all hopping rates in the chain [60]. The diffusion coefficient $D(F,T)$ can be determined numerically by generating random chains with the desired distribution of site energies and then evaluating Derrida's expression for the chain as described in Section 3.6.

The problem can also be solved analytically. Derrida derived the limits of his expressions for an infinitely long chain, in terms of various expectation values containing the jump rates. However these expressions are applicable only when the jump rates between different pairs of sites are not correlated. This condition is not satisfied for the Miller–Abrahams hopping rates we consider: there is a correlation between the rates of the two consecutive hops $\Gamma_{i-1,i}$ and $\Gamma_{i,i+1}$, since they both depend on the energy ε_i of the shared site i.

Bouchaud and Georges [80] studied a chain of sites separated by the distance d, where the hopping rates are given by the so-called random barrier model:

$$\Gamma_{i,i\pm1} = \Gamma_0 \exp\left[\frac{\Delta_{i\pm1,i} \pm eFd}{2kT}\right]. \tag{6.4}$$

Here the barrier heights $\Delta_{i,i+1} = \Delta_{i+1,i}$ have a Gaussian distribution, given by

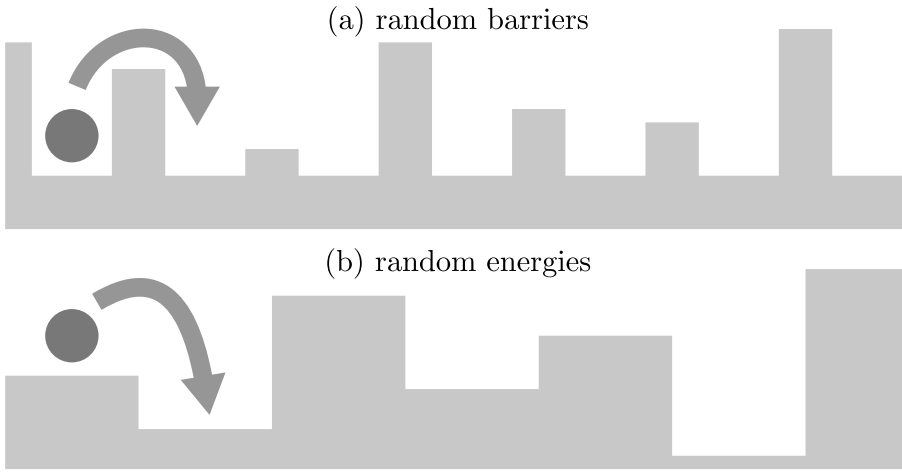

FIGURE 6.2 Illustration of (a) the random barrier model where all sites have the same energy, but are separated by barriers with random heights, and (b) the random energy model where the site energies are random and the Miller–Abrahams hopping rates are used.

Eq. (1.8). The difference between the Miller–Abrahams rate and the random barrier model is illustrated in Fig. 6.2. In the random barrier model, sequential jumps are not correlated and hence Derrida's expressions for infinite chains can be applied. Bouchaud and Georges derived an expression for $D(F,T)$, showing a linear dependence of D on F (for small fields). The expression given in Ref. 80 is misprinted, but the correct version given in Paper IV also demonstrates a linear field dependence.

For the case of Miller–Abrahams hopping rates, a different approach is necessary. In deriving the expressions for an infinite chain, Derrida defined the diffusion coefficient microscopically with Eq. (6.1). In order to obtain an expression for D valid for the Miller–Abrahams hopping rate we proceed in a different way, using a macroscopic definition of D. We define the diffusion coefficient in terms of the diffusion current j_D created by a long-range gradient of the average electron concentration $n(x)$, as illustrated in Fig. 6.3.

$$D = -\frac{j_D(x)}{dn(x)/dx}, \tag{6.5}$$

From here an expression for $D(F,T)$ was derived. This rather complicated ex-

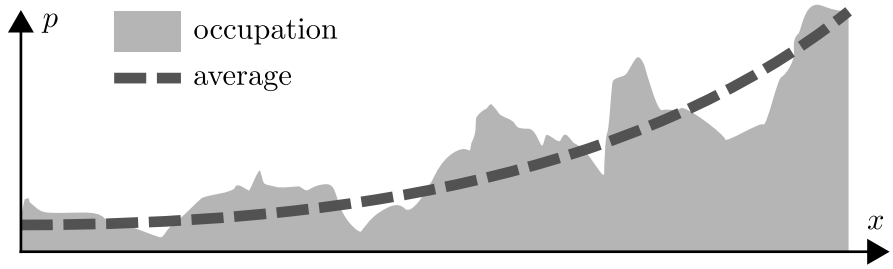

FIGURE 6.3 The diffusion coefficient is determined from the response of the system to a gradient of the average concentration. The shaded area represents the electron concentration on individual sites, which varies due to the random site energies. The dashed curve represents the concentration averaged over many sites.

pression, given in Paper IV, can be approximated for small temperatures and fields, $|eFd| < kT \ll \sigma$ as

$$D(F) \approx \frac{d^2}{2A} + \frac{|Fe|d^3}{2kT} + \frac{F^2e^2d^4A}{8(kT)^2} + \frac{|Fe|^3d^5A}{16(kT)^3}, \tag{6.6}$$

where $A = \exp\left(\sigma^2/(kT)^2\right)$. Under the same conditions, the mobility can be approximated as

$$\mu(F) \approx \frac{ed^2}{2AkT} + \frac{|Fe|ed^3}{4A(kT)^2} + \frac{F^2e^3d^4}{12A(kT)^3} \tag{6.7}$$

From these expressions we see that also for Miller–Abrahams rates both the diffusion coefficient and the mobility contain a term that is linear in the field.

Since both the analytical result and the derivation of it are complicated, and since it is not trivial to show that the two definitions of the diffusion coefficient are equivalent, it is useful to compare the analytical expression for $D(F,T)$ with numerical results. To obtain numerical results, we generated chains of sites with random energies. We then evaluated the mobility and diffusion coefficients in these chains, using Derrida's equations (3.18) and (3.19). To obtain consistent results between different realizations of the random energies, extremely long chains were needed. The numerical results in Paper IV were obtained for chains of 10^7 and 10^8 sites. This is the point were the fast algorithm given in Section 3.6 becomes important. Evaluating the expressions directly in $O(N^2)$ steps would

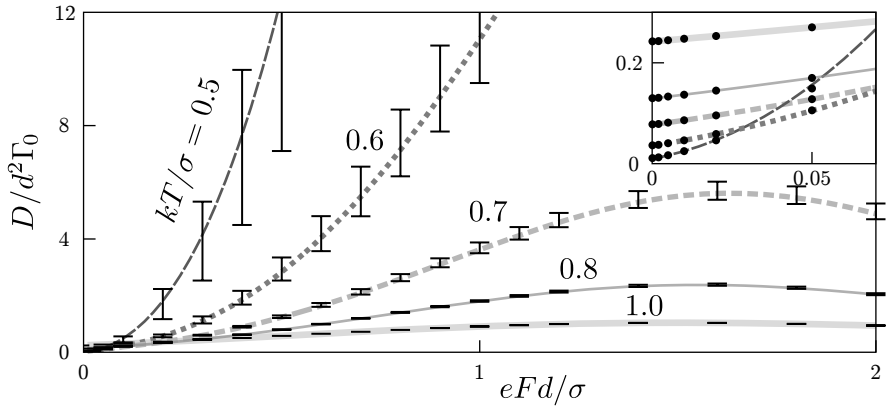

FIGURE 6.4 Diffusion coefficient in one dimension as a function of the electric field. The curves show the analytical solution, while the symbols show numerical results for chains with 10^8 sites.

simply not be practical. Fig. 6.4 shows a satisfying agreement between the analytical and numerical results for the field dependence of the diffusion coefficient. Note that the spread in the numerical results are larger for the lower temperatures. The same behavior is found for two- and three-dimensional systems: the lower the temperature is, the larger are the variation in diffusion coefficient between different realizations and the larger must the system be in order to obtain reliable results. The requirements on system size are investigated further in the following sections.

6.3 Diffusion in two and three dimensions

In two and three dimensions, the diffusion coefficient D in the direction of the field was found to depend quadratically on the field strength. This result is based on Monte Carlo simulations (Chapter 2) and an approximate analytical treatment based on the multiple trapping approach of Rudenko and Arkhipov [15]. The simulations show that D has a stronger field dependence than the mobility μ, and that D depends on the field at such low fields that the mobility is nearly constant, see Fig. 6.5a. In three dimensions, one can also determine the diffusion coefficient in the plane perpendicular to the field's direction. The transversal diffusion coefficient is as expected equal to the longitudinal one in

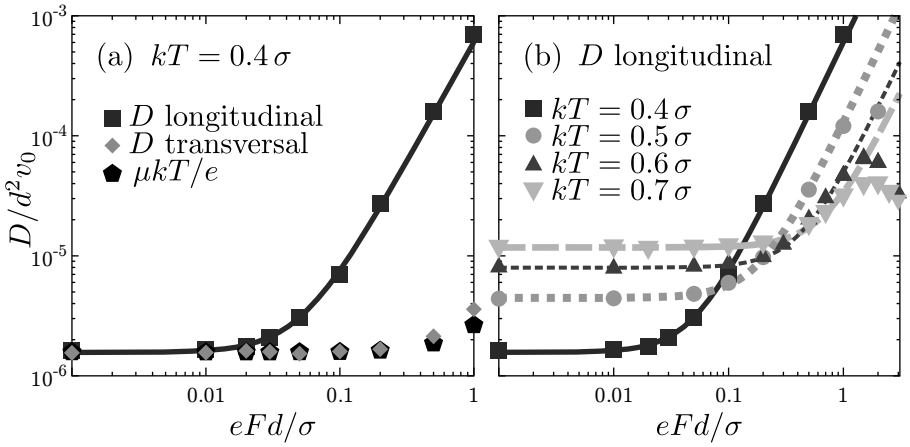

FIGURE 6.5 Simulation results for a three-dimensional system. (a) The diffusion coefficient along and perpendicular to the field, together with the mobility (scaled with kT/e to show where Einstein's relation (6.3) is valid). (b) The diffusion coefficient along the field, for several temperatures. The curves show the best fits to $D(F,T) = D_0(T) + A(T)F^2$. The system is a cubic lattice of 700^3 sites with lattice constant d and localization length $0.2d$.

the small-field limit, but increases slower when the field is increased, as shown in Fig. 6.5a. The diffusion coefficient along the field is shown in Fig. 6.5b for different temperatures. For all temperatures tested, D depends quadratically on the field, with a steeper dependence for lower temperatures. No evidence for a term linear in F could be found in the simulation results for $D(F,T)$.

6.4 Multiple trapping

In the multiple trapping model of Rudenko and Arkhipov [15], electrons either move freely in the conduction band (with a known mobility) or are trapped. No hopping events from one trap to another are considered, instead it is assumed that the electrons in a trap can move only when they are excited to the conduction band. From the rates of electron trapping and electron release, one obtains the properties of the electron's motion, i.e. the mobility and diffusion coefficient. A similar model can be applied to determining the diffusion coefficient for the hopping transport process, if the following assumption is true: The field dependence of the diffusion coefficient in hopping transport is determined by trapping at very rare low-energy sites. The assumption is justified by simulation results given below. We treat the rare low-energy sites as traps in the multiple trapping sense, and treat the electrons as free when they are not trapped at the low-energy sites. An important additional assumption is that sequential trapping events are not correlated. This assumption seems reasonable in two and three dimensions, but not in one dimension, where there is a significant probability for an electron to return to an already visited trap.

Since the details of the multiple trapping-like approach are given in Paper V, I do not repeat them, but just state some important conclusions. If the system is symmetric, so that the directions x and $-x$ are equivalent, there is no linear term in $D(F)$. The diffusion coefficient depends on field and temperature as

$$D(F,T) = D_0(T) + A(T)F^2. \tag{6.8}$$

The function $A(T)$ can be obtained from the multiple trapping considerations, but only in terms of other quantities that have to be determined numerically. The most important result of the multiple trapping, besides the quadratic field dependence of D, is that one can determine the energy of the traps that contribute the most to the diffusion coefficient.

6.5 The sites that determine the diffusion coefficient

While the mobility is determined by sites in the vicinity of the average electron energy $\langle\varepsilon\rangle = -\sigma^2/kT$, the multiple trapping approach shows that the sites important for diffusion are situated around $\varepsilon^* = -2\sigma^2/kT$, much deeper in the low-energy tail of the density of states. This prediction was verified in a Monte Carlo simulation (Fig. 4 in Paper V), where all sites below a cut-off energy ε_c were replaced by sites with a higher energy, chosen randomly. The diffusion coefficient and the mobility were then calculated for the same system for different values of ε_c. The diffusion coefficient was affected when sites around ε^* were removed, while the mobility remained constant until the ε_c came close to $\langle\varepsilon\rangle$. This result is significant for simulations, since to obtain correct results one must simulate a system so large that the important sites around ε^* are present and well represented. Since ε^* depends on the temperature, one can also say that the simulation results for a fixed system size are reliable only for temperatures above some critical temperature that depends on the system size. For this reason we wanted to simulate as large systems as possible and thus chose to use the lattice Monte Carlo method described in Chapter 2. We simulated systems containing $700^3 = 3.43 \cdot 10^8$ sites, and found that the diffusion results were reliable for temperatures $kT \gtrsim 0.33\sigma$.

6.6 Why is the Einstein relation broken?

In both the analytical and the numerical results presented here, it is seen that Einstein's relation between the electron mobility and diffusion coefficient is valid only in the low-field limit. This behavior has also been reported before, based on simulation studies [28, 29, 81]. Let us conclude the discussion of diffusion with a suggestion as to why this is the case.

Einstein's relation is derived for a finite, closed system in a steady state, where no net current flows [79]. The system is subjected to an external electric field, which causes a gradient in the electron concentration. The relation is obtained by demanding that the current due to drift and the current due to diffusion sum to zero. We consider, however, a system with periodic boundary conditions, where there is a net current in the steady state, if an electric field is applied. As this breaks one of the assumptions in the derivation, it is perhaps not so surprising that our systems do not obey the Einstein relation when an electric field is applied.

Chapter 7

Recombination and diffusion

In the preceding chapters we have discussed transport of first single charge carriers, then several charge carriers simultaneously, and several charge carriers with Coulomb interaction taken into account. However, so far we have considered systems where only electrons or only holes are present. If both electrons and holes are present simultaneously in a material, one more effect is possible, namely recombination of electrons and holes. The topic of this chapter, and of Paper VI, is how diffusion influences the charge carrier recombination process.

Two practical applications where recombination is important are light emitting diodes and solar cells. In light emitting diodes, light is generated when electrons and holes recombine, thus it is desirable to have as efficient recombination as possible (and that the recombination is radiative). In solar cells, incoming light creates electrons and holes. If the electrons and holes reach their respective contact they contribute to the current generated by the solar cell. If they instead recombine inside the device they are lost. Thus recombination decreases the conversion efficiency in a solar cell, and is not desired.

There has been a lot of interest in modeling recombination in organic solar cells, especially in the so-called bulk heterojunction solar cells. In these devices, the active layer consists of a mixture of two materials, one of which transports electrons, while the other one transports holes. Recombination in organic solar cells is frequently described using Langevin's model [82, 83]. However, experiments on these devices show that the recombination rate in them is slower (by several orders of magnitude) than what is predicted by Langevin's equation. The reason for this deviation is not well understood. In general it seems that a high conversion efficiency correlates with a low recombination rate. Good solar cells have been made by using the conductive polymer regio-

regular poly(3-hexylthiophene), RR-P3HT, as the hole-transporting material, often together with the fullerene derivative PCBM as electron transporter. Juška et al. suggested [82, 83] that since RR-P3HT is anisotropic, it behaves like a two-dimensional material. They then derived the recombination rate for a two-dimensional version of Langevin's model, and found it to be much lower than in the three-dimensional case (over two orders of magnitude lower, at typical conditions).

In transferring Langevin's theory from three dimensions to two, there is a subtle problem related to charge carrier diffusion. Langevin's model considers only the drift motion of charge carriers, while the diffusion is ignored. In a three-dimensional system this is justified, since, as we will see below, diffusion plays no role for recombination in three dimensions. For recombination in two dimensions, however, the situation is different. In a two-dimensional system, there will be a net current due to diffusion in addition to the drift current. This diffusion current will increase the recombination rate, above the value obtained by considering only the current due to drift. The smaller the charge carrier concentration is, the larger is the contribution from diffusive motion to the recombination rate.

The rest of this chapter is organized as follows. Section 7.1 briefly describes Langevin's model for recombination in three dimensions. In Section 7.2, the recombination rate for a two-dimensional system is derived, with the diffusion process taken into account. It is shown, that the result of Juška et al. is obtained as a limiting case, in the limit of high charge carrier concentration.

7.1 Langevin's model

Langevin studied the recombination of positive and negative particles by considering one particle of each kind, drifting towards each other because of Coulomb attraction. In our case the particles are electrons and holes. Langevin's model assumes that the motion of electrons and holes can be described by (field independent) mobilities. If the electron has the mobility μ_e and the hole has the mobility μ_h, their velocities (toward each other) are $v_e = \mu_e F(r)$ and $v_h = \mu_h F(r)$, respectively. The magnitude $F(r)$ of the electric field from the other charge carrier is

$$F(r) = \frac{1}{4\pi\varepsilon\varepsilon_0}\frac{1}{r^2}. \tag{7.1}$$

One can now calculate the time required for the electron and hole to meet given the starting distance r_0, which can be estimated from the concentrations of

electrons and holes. The concentrations N_e of electrons and N_h of holes are assumed to be equal, $N_e = N_h$. The recombination time is

$$t = \frac{\varepsilon\varepsilon_0}{(\mu_e + \mu_h)e} N_e \tag{7.2}$$

and the recombination rate per unit volume is then [82–84]

$$\mathcal{R}_{\text{rec}} = \frac{N_e}{t} = \frac{(\mu_e + \mu_h)e}{\varepsilon\varepsilon_0} N_e^2. \tag{7.3}$$

The model assumes that the system is continuous. Nevertheless, it can be expected to work also for hopping transport, provided that typical hopping distances are shorter than the length scale of the model, given by the (zero-field) Onsager radius. The Onsager radius

$$r_{\text{O}} = \frac{e^2}{4\pi\varepsilon\varepsilon_0 kT} \tag{7.4}$$

is defined as the separation between an electron and a hole, at which the Coulomb energy of the pair equals kT.

In the derivation above, diffusion was not taken into account. In three dimensions this is correct [84], which can be seen by calculating the flux of electrons through a spherical surface of radius r centered at a fixed hole. The electric field from the hole scales as r^{-2}, while the surface area of the sphere scales as r^2. Thus there is a steady state where the electron concentration is independent of the distance to the hole. When there are no concentration gradients there will be no diffusion currents, thus diffusion can be ignored in the three-dimensional case.

In a two-dimensional system, a similar consideration of the electron flow through a circle of radius r shows that the electron concentration must be r-dependent in order to have the same flux of electrons at different radii. Contributions from diffusion should then be taken into account [84], as discussed in the following section.

7.2 Recombination in two dimensions

Juška et al. repeated the derivation leading to Langevin's expression (7.3) for the case of a two-dimensional material, taking only drift into account and ignoring diffusion [82, 83]. The recombination time and rate are then

$$t^{\text{2D}} = \frac{4}{3\sqrt{\pi}} \frac{\varepsilon\varepsilon_0}{(\mu_e + \mu_h)e} N_e^{-3/2}, \qquad \mathcal{R}_{\text{rec}}^{\text{2D}} = \frac{3\sqrt{\pi}}{4} \frac{(\mu_e + \mu_h)e}{\varepsilon\varepsilon_0} N_e^{5/2}. \tag{7.5}$$

However, as stated above, diffusion can in general not be ignored in a two-dimensional system. To study the recombination process when the charge carriers diffuse as well as drift, we consider the following model by Greenham and Bobbert [84]. Electrons are generated uniformly with the fixed rate f inside a circle with radius R, centered on a fixed hole. The radius is chosen so that

$$\frac{1}{\pi R^2} = N_h. \tag{7.6}$$

The electrons move due to diffusion and drift. The hole acts as a sink for the electrons, so that the electrons disappear when they reach the hole. This model is solved in terms of the electron concentration $n(\boldsymbol{r})$ and the current $\boldsymbol{J}(\boldsymbol{r})$. The current is determined by

$$\boldsymbol{J}(\boldsymbol{r}) = -\mu\, n(\boldsymbol{r})\, \boldsymbol{E}(\boldsymbol{r}) - D\, \nabla n(\boldsymbol{r}), \tag{7.7}$$

where μ is the mobility and D is the diffusion coefficient of the electrons. Since the hole is fixed in this model, we assume that the electrons move with the combined mobility of both charge carrier types: $\mu = \mu_h + \mu_e$. Additionally, continuity gives

$$\nabla \cdot \boldsymbol{J}(\boldsymbol{r}) = f. \tag{7.8}$$

The recombination time is then obtained as

$$t = \frac{\langle n(\boldsymbol{r}) \rangle}{f} \tag{7.9}$$

where $\langle n(\boldsymbol{r}) \rangle$ is the electron concentration averaged over the area inside the circular boundary. The equations given above can be solved analytically (assuming that Einstein's relation between μ and D holds), and the recombination time expressed using the Meijer G function:

$$t = \frac{r_\mathrm{O}^2}{D} \left(\frac{R^2}{r_\mathrm{O}^2} - \frac{1}{2} \right) G_{23}^{31}\left(\frac{r_\mathrm{O}}{R} \,\middle|\, \begin{matrix} 0, 3 \\ 0, 0, 2 \end{matrix} \right) + \frac{R}{6 r_\mathrm{O}} - \frac{R^2}{8 r_\mathrm{O}^2}. \tag{7.10}$$

In order to compare this result to Eq. (7.5) obtained by Juška et al., we will examine the limiting cases of high and low concentration. We obtain the limits by series expansion of the G function. In the limit of a high carrier concentration we obtain

$$t = \frac{8}{15\sqrt{\pi}} \frac{\varepsilon \varepsilon_0}{e \mu} N_e^{-3/2}, \tag{7.11}$$

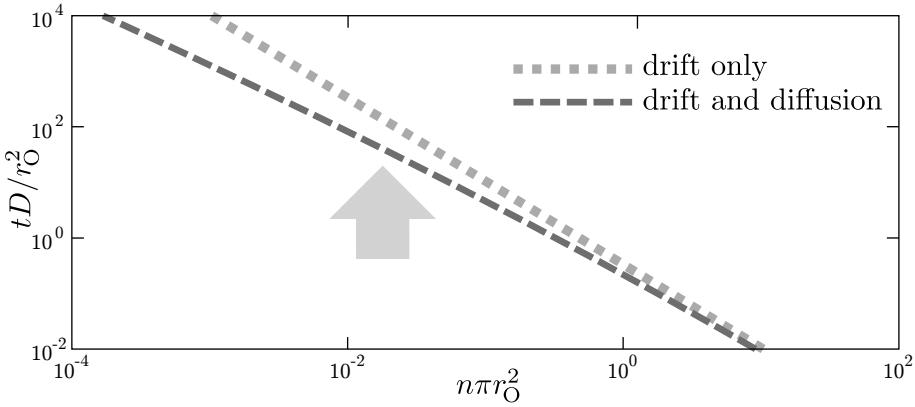

FIGURE 7.1 The recombination time t as a function of the charge carrier concentration n. The concentration is measured by the number of charge carriers inside the Onsager radius r_O. The arrow indicates a charge carrier concentrations typical for experiments [82, 83].

identical to the result (7.5) obtained in the absence of diffusion apart from a factor 2/5. In Paper VI it is shown that if the model is modified so that all electrons start at the periphery of the circle instead of uniformly spread over its area, the result is identical to Juška's result (7.5) in the high concentration limit. Thus the contribution of diffusion to the recombination rate can be ignored in the case of a high charge carrier concentration. In the limit of low carrier concentration, the model with drift and diffusion gives a different expression for the recombination time,

$$t = \frac{1}{4\pi D}\frac{1}{N_e}\log\frac{1}{e^{2\gamma+3/2}\pi r_O^2 N_e}. \tag{7.12}$$

were $\gamma = 0.577...$ is Euler's constant.

The recombination time calculated in the two models are shown in Fig. 7.1 as functions of the charge carrier concentration. The two models agree in the high concentration limit. The recombination time is shorter in the model that includes diffusion and the difference increases with decreasing carrier concentration. The critical concentration, above which diffusion can be neglected, is roughly $1/(\pi r_O^2)$, corresponding to one particle within the Onsager radius. Charge carrier concentrations in experiments are typically less than this value, typical experimental conditions [82, 83] are indicated by the arrow in Fig. 7.1.

Ignoring the diffusion increases the recombination time by a factor three at these conditions, showing that the contribution from diffusion has a practical relevance and not just a theoretical one. However, the idea of Juška et al., that the anisotropic conductivity in RR-P3HT causes the recombination rate to be lower than predicted by Langevin's three-dimensional model may still be valid. Even when diffusion is taken into account, the recombination rate in a two-dimensional system is still slower by roughly a factor 50 than in a three-dimensional one, at the parameters considered in Refs. 82 and 83.

Bibliography

[1] F. Jansson, S. D. Baranovskii, G. Sliaužys, R. Österbacka, and P. Thomas, "Effective temperature for hopping transport in a Gaussian DOS," Phys. Status Solidi C **5**, 722 (2008).

[2] F. Jansson and R. Österbacka, "Simulation of double injection in a bulk heterojunction material using the Gaussian disorder model," Phys. Status Solidi C **5**, 755 (2008).

[3] A. Laiho, H. S. Majumdar, J. K. Baral, F. Jansson, R. Österbacka, and O. Ikkala, "Tuning the electrical switching of polymer/fullerene nanocomposite thin film devices by control of morphology," Appl. Phys. Lett. **93**, 203309 (2008).

[4] F. Jansson, A. V. Nenashev, S. D. Baranovskii, F. Gebhard, and R. Österbacka, "Effect of electric field on diffusion in disordered materials," Ann. Phys. (Berlin) **18**, 856 (2009).

[5] S. D. Baranovskii, O. Rubel, F. Jansson, and R. Österbacka, *Advances in Polymer Science 223: Organic Electronics, edited by G. Meller and T. Grasser* (Springer, Heidelberg, 2010), chap. Description of Charge Transport in Disordered Organic Materials.

[6] R. Pörn, O. Nissfolk, F. Jansson, and T. Westerlund, "The Coulomb Glass—Modeling and Computational Experience with a Large Scale 0–1 QP Problem," to appear in the proceedings of ESCAPE 21 in Computer Aided Chemical Engineering (2011).

[7] M. Wiemer, A. V. Nenashev, F. Jansson, and S. D. Baranovskii, "On the efficiency of exciton dissociation at the interface between a conjugated polymer and an electron acceptor," accepted by Appl. Phys. Lett. (2011).

[8] A. V. Nenashev, S. D. Baranovskii, M. Wiemer, F. Jansson, R. Österbacka, A. V. Dvurechenskii, and F. Gebhard, "Theory to exciton dissociation at the interface between a conjugated polymer and an electron acceptor," submitted to Phys. Rev. B (2011).

[9] S. Baranovski, ed., *Charge Transport in Disordered Solids with Applications in Electronics* (John Wiley & Sons, Ltd, Chichester, 2006).

[10] A. Miller and E. Abrahams, "Impurity conduction at low concentrations," Phys. Rev. **120**, 745 (1960).

[11] V. Ambegaokar, B. I. Halperin, and J. S. Langer, "Hopping conductivity in disordered systems," Phys. Rev. B **4**, 2612 (1971).

[12] J. H. Slowik and I. Chen, "Effect of molecular rotation upon charge transport between disordered carbazole units," J. Appl. Phys. **54**, 4467 (1983).

[13] H. Bässler, "Charge transport in disordered organic photoconductors—a Monte Carlo simulation study," Phys. Status Solidi B **175**, 15 (1993).

[14] P. M. Borsenberger, E. H. Magin, M. van der Auweraer, and F. C. de Schryver, "The role of disorder on charge transport in molecularly doped polymers and related materials," Phys. Status Solidi A **140**, 9 (1993).

[15] A. I. Rudenko and V. I. Arkhipov, "Drift and diffusion in materials with traps," Philos. Mag. B **45**, 177 (1982).

[16] Yu. N. Gartstein and E. M. Conwell, "High-field hopping mobility in molecular systems with spatially correlated energetic disorder," Chem. Phys. Lett. **245**, 351 (1995).

[17] D. H. Dunlap, P. E. Parris, and V. M. Kenkre, "Charge-dipole model for the universal field dependence of mobilities in molecularly doped polymers," Phys. Rev. Lett. **77**, 542 (1996).

[18] S. V. Novikov, D. H. Dunlap, V. M. Kenkre, P. E. Parris, and A. V. Vannikov, "Essential role of correlations in governing charge transport in disordered organic materials," Phys. Rev. Lett. **81**, 4472 (1998).

[19] S. V. Novikov, "Organic glasses: cluster structure of the random energy landscape," Ann. Phys. (Berlin) **18**, 949 (2009).

[20] R. A. Marcus and N. Sutin, "Electron transfers in chemistry and biology," Biochim. Biophys. Acta **811**, 265 (1985).

[21] B. I. Shklovskii and A. L. Efros, *Electronic Properties of Doped Semiconductors* (Springer-Verlag, 1984).

[22] M. C. J. M. Vissenberg and M. Matters, "Theory of the field-effect mobility in amorphous organic transistors," Phys. Rev. B **57**, 12964 (1998).

[23] M. Grünewald and P. Thomas, "A hopping model for activated charge transport in amorphous silicon," Phys. Status Solidi B **94**, 125 (1979).

[24] D. Monroe, "Hopping in exponential band tails," Phys. Rev. Lett. **54**, 146 (1985).

[25] J. O. Oelerich, D. Huemmer, M. Weseloh, and S. D. Baranovskii, "Concentration dependence of the transport energy level for charge carriers in organic semiconductors," Appl. Phys. Lett. **97**, 143302 (2010).

[26] M. Silver, K. S. Dy, and I. L. Huang, "Monte Carlo calculation of the transient photocurrent in low-carrier-mobility materials," Phys. Rev. Lett. **27**, 21 (1971).

[27] G. Schönherr, H. Bässler, and M. Silver, "Dispersive hopping transport via sites having a Gaussian distribution of energies," Philos. Mag. B **44**, 47 (1981).

[28] R. Richert, L. Pautmeier, and H. Bässler, "Diffusion and drift of charge carriers in a random potential: Deviation from Einstein's law," Phys. Rev. Lett. **63**, 547 (1989).

[29] L. Pautmeier, R. Richert, and H. Bässler, "Anomalous time-independent diffusion of charge carriers in a random potential under a bias field," Philos. Mag. B **63**, 587 (1991).

[30] D. T. Gillespie, "A general method for numerically simulating the stochastic time evolution of coupled chemical reactions," J. Comput. Phys. **22**, 403 (1976).

[31] D. T. Gillespie, "Exact stochastic simulation of coupled chemical reactions," J. Phys. Chem. **81**, 2340 (1977).

[32] J. Thijssen, *Computational Physics* (Cambridge University Press, 2007), 2nd ed.

[33] M. E. J. Newman and G. T. Barkema, *Monte Carlo methods in statistical physics* (Oxford University Press, USA, 1999).

[34] A. Hirao, H. Nishizawa, and M. Sugiuchi, "Diffusion and drift of charge carriers in molecularly doped polymers," Phys. Rev. Lett. **75**, 1787 (1995).

[35] H. Cordes, S. D. Baranovskii, K. Kohary, P. Thomas, S. Yamasaki, F. Hensel, and J.-H. Wendorff, "One-dimensional hopping transport in disordered organic solids. I. Analytic calculations," Phys. Rev. B **63**, 094201 (2001).

[36] A. M. Somoza and M. Ortuño, "Monte Carlo method for relaxation in electron glasses," Phys. Rev. B **72**, 224202 (2005).

[37] M. Ortuño, M. Caravaca, and A. M. Somoza, "Numerical study of relaxation in Coulomb glasses," Phys. Status Solidi C **5**, 674 (2008).

[38] S. D. Baranovskii, B. Cleve, R. Hess, and P. Thomas, "Effective temperature for electrons in band tails," J. Non-Cryst. Solids **164-166**, 437 (1993).

[39] J. Zhou, Y. C. Zhou, J. M. Zhao, C. Q. Wu, X. M. Ding, and X. Y. Hou, "Carrier density dependence of mobility in organic solids: A Monte Carlo simulation," Phys. Rev. B **75**, 153201 (2007).

[40] J. Zhou, Y. C. Zhou, X. D. Gao, C. Q. Wu, X. M. Ding, and X. Y. Hou, "Monte Carlo simulation of charge transport in electrically doped organic solids," J. Phys. D **42**, 035103 (2009).

[41] S. V. Novikov, "Hopping transport of interacting carriers in disordered organic materials," Phys. Status Solidi C **5**, 740 (2008).

[42] M. Pollak, "Effect of carrier–carrier interactions on some transport properties in disordered semiconductors," Discuss. Faraday Soc. **50**, 13 (1970).

[43] D. N. Tsigankov, E. Pazy, B. D. Laikhtman, and A. L. Efros, "Long-time relaxation of interacting electrons in the regime of hopping conduction," Phys. Rev. B **68**, 184205 (2003).

[44] A. Amir, Y. Oreg, and Y. Imry, "Mean-field model for electron-glass dynamics," Phys. Rev. B **77**, 165207 (2008).

[45] M. A. Gibson and J. Bruck, "Efficient exact stochastic simulation of chemical systems with many species and many channels," J. Phys. Chem. A **104**, 1876 (2000).

[46] A. Slepoy, A. P. Thompson, and S. J. Plimpton, "A constant-time kinetic Monte Carlo algorithm for simulation of large biochemical reaction networks," J. Chem. Phys. **128**, 205101 (2008).

[47] J. J. Lukkien, J. P. L. Segers, P. A. J. Hilbers, R. J. Gelten, and A. P. J. Jansen, "Efficient Monte Carlo methods for the simulation of catalytic surface reactions," Phys. Rev. E **58**, 2598 (1998).

[48] A. J. Walker, "New fast method for generating discrete random numbers with arbitrary frequency distributions," Electron. Lett. **10**, 127 (1974).

[49] A. J. Walker, "An efficient method for generating discrete random variables with general distributions," ACM Trans. Math. Softw. **3**, 253 (1977).

[50] D. E. Knuth, *The art of computer programming, volume 2 (3rd ed.): Seminumerical algorithms* (Addison-Wesley Longman Publishing Co., Inc., Boston, MA, USA, 1997).

[51] W. H. Press, S. A. Teukolsky, W. T. Vetterling, and B. P. Flannery, *Numerical recipes in C (2nd ed.): the art of scientific computing* (Cambridge University Press, New York, 1992).

[52] M. Matsumoto and T. Nishimura, "Mersenne twister: a 623-dimensionally equidistributed uniform pseudo-random number generator," ACM Trans. Model. Comput. Simul. **8**, 3 (1998).

[53] Z. G. Yu, D. L. Smith, A. Saxena, R. L. Martin, and A. R. Bishop, "Molecular geometry fluctuation model for the mobility of conjugated polymers," Phys. Rev. Lett. **84**, 721 (2000).

[54] Z. G. Yu, D. L. Smith, A. Saxena, R. L. Martin, and A. R. Bishop, "Molecular geometry fluctuations and field-dependent mobility in conjugated polymers," Phys. Rev. B **63**, 085202 (2001).

[55] W. F. Pasveer, J. Cottaar, C. Tanase, R. Coehoorn, P. A. Bobbert, P. W. M. Blom, D. M. de Leeuw, and M. A. J. Michels, "Unified description of charge-carrier mobilities in disordered semiconducting polymers," Phys. Rev. Lett. **94**, 206601 (2005).

[56] J. Cottaar and P. A. Bobbert, "Calculating charge-carrier mobilities in disordered semiconducting polymers: Mean field and beyond," Phys. Rev. B **74**, 115204 (2006).

[57] S. Marianer and B. I. Shklovskii, "Effective temperature of hopping electrons in a strong electric field," Phys. Rev. B **46**, 13100 (1992).

[58] W. F. Pasveer, P. A. Bobbert, H. P. Huinink, and M. A. J. Michels, "Scaling of current distributions in variable-range hopping transport on two- and three-dimensional lattices," Phys. Rev. B **72**, 174204 (2005).

[59] G. Engeln-Müllges and F. Uhlig, *Numerical algorithms with C* (Springer-Verlag, Berlin, 1996).

[60] B. Derrida, "Velocity and diffusion constant of a periodic one-dimensional hopping model," J. Stat. Phys **31**, 433 (1983).

[61] B. I. Shklovskii, "Hopping conduction in semiconductors in a strong electric field," Sov. Phys. Semicond. **6**, 1964 (1973).

[62] B. Cleve, B. Hartenstein, S. D. Baranovskii, M. Scheidler, P. Thomas, and H. Bässler, "High-field hopping transport in band tails of disordered semiconductors," Phys. Rev. B **51**, 16705 (1995).

[63] N. Vukmirović and L.-W. Wang, "Carrier heating in disordered conjugated polymers in electric field," Phys. Rev. B **81**, 035210 (2010).

[64] E. Tutiš, I. Jurić, and I. Batistić, "Particle-energy distribution and effective temperature for the hopping transport in one-dimensional disordered system," Croat. Chem. Acta **83**, 87 (2010).

[65] I. Jurić, I. Batistić, and E. Tutiš, "Beyond the effective temperature: The electron ensemble at high electric fields in disordered organics," Phys. Rev. B **82**, 165205 (2010).

[66] L. Esaki, "New phenomenon in narrow germanium p–n junctions," Phys. Rev. **109**, 603 (1958).

[67] J. G. Simmons and R. R. Verderber, "New conduction and reversible memory phenomena in thin insulating films," Proc. R. Soc. London A **301**, 77 (1967).

[68] R. E. Thurstans and D. P. Oxley, "The electroformed metal–insulator–metal structure: a comprehensive model," J. Phys. D **35**, 802 (2002).

[69] L. D. Bozano, B. W. Kean, V. R. Deline, J. R. Salem, and J. C. Scott, "Mechanism for bistability in organic memory elements," Appl. Phys. Lett. **84**, 607 (2004).

[70] L. D. Bozano, B. W. Kean, M. Beinhoff, K. R. Carter, P. M. Rice, and J. C. Scott, "Organic materials and thin-film structures for cross-point memory cells based on trapping in metallic nanoparticles," Adv. Funct. Mater. **15**, 1933 (2005).

[71] H. S. Majumdar, J. K. Baral, R. Österbacka, O. Ikkala, and H. Stubb, "Fullerene-based bistable devices and associated negative differential resistance effect," Org. Electron. **6**, 188 (2005).

[72] S. Paul, A. Kanwal, and M. Chhowalla, "Memory effect in thin films of insulating polymer and C_{60} nanocomposites," Nanotechnology **17**, 145 (2006).

[73] J. C. Scott and L. D. Bozano, "Nonvolatile memory elements based on organic materials," Adv. Mater. **19**, 1452 (2007).

[74] F. Verbakel, S. C. J. Meskers, R. A. J. Janssen, H. L. Gomes, M. Colle, M. Buchel, and D. M. de Leeuw, "Reproducible resistive switching in nonvolatile organic memories," Appl. Phys. Lett. **91**, 192103 (2007).

[75] J. K. Baral, H. S. Majumdar, A. Laiho, H. Jiang, E. I. Kauppinen, R. H. A. Ras, J. Ruokolainen, O. Ikkala, and R. Österbacka, "Organic memory using [6,6]-phenyl-C_{61} butyric acid methyl ester: morphology, thickness and concentration dependence studies," Nanotechnology **19**, 035203 (2008).

[76] Nguyen Van Lien and B. I. Shklovskii, "Hopping conduction in strong electric fields and directed percolation," Solid State Commun. **38**, 99 (1981).

[77] Yu. N. Gartstein, S. Jeyadev, and E. M. Conwell, "Monte Carlo simulation of high-field hopping on a bond-disordered lattice," Phys. Rev. B **51**, 4622 (1995).

[78] M. Shin, S. Lee, K. W. Park, and E.-H. Lee, "Secondary Coulomb blockade gap in a four-island tunnel-junction array," Phys. Rev. B **59**, 3160 (1999).

[79] R. P. Feynman, R. B. Leighton, and M. Sands, *The Feynman Lectures on Physics*, vol. 1 (Addison-Wesley, Reading Massachusetts, 1963).

[80] J. P. Bouchaud and A. Georges, "Comment on ''Diffusion and drift of charge carriers in a random potential: Deviation from Einstein's law'','' Phys. Rev. Lett. **63**, 2692 (1989).

[81] J. M. Casado and J. J. Mejías, "Charge transport for a class of conducting polymers: The dependence of the mobility on applied fields," Philos. Mag. B **70**, 1111 (1994).

[82] G. Juška, K. Genevičius, N. Nekrašas, G. Sliaužys, and R. Österbacka, "Two dimensional Langevin recombination in regioregular poly(3-hexylthiophene)," Appl. Phys. Lett. **95**, 013303 (2009).

[83] G. Juška, K. Genevičius, N. Nekrašas, and G. Sliaužys, "Two-dimensional Langevin recombination," Phys. Status Solidi C **7**, 980 (2010).

[84] N. C. Greenham and P. A. Bobbert, "Two-dimensional electron–hole capture in a disordered hopping system," Phys. Rev. B **68**, 245301 (2003).

Svensk resumé

Min avhandling behandlar hur oordnade material leder elektrisk ström. Bland materialen som studeras finns ledande polymerer, d.v.s. plaster som leder ström, och mer allmänt organiska halvledare. Av de här materialen har man kunnat bygga elektroniska komponenter, och man hoppas på att kunna trycka hela kretsar av organiska material.

För de här tillämpningarna är det viktigt att förstå hur materialen själva leder elektrisk ström. Termen oordnade material syftar på material som saknar kristallstruktur. Oordningen gör att elektronernas tillstånd blir lokaliserade i rummet, så att en elektron i ett visst tillstånd är begränsad t.ex. till en molekyl eller ett segment av en polymer. Det här kan jämföras med kristallina material, där ett elektrontillstånd är utspritt över hela kristallen (men i stället har en väldefinierad rörelsemängd). Elektronerna (eller hålen) i det oordnade materialet kan röra sig genom att tunnelera mellan de lokaliserade tillstånden. Utgående från egenskaperna för den här tunneleringsprocessen, kan man bestämma transportegenskaperna för hela materialet. Det här är utgångspunkten för den så kallade hopptransportmodellen, som jag har använt mig av. Hopptransportmodellen innehåller flera drastiska förenklingar. Till exempel betraktas elektrontillstånden som punktformiga, så att tunneleringssannolikheten mellan två tillstånd endast beror på avståndet mellan dem, och inte på deras relativa orientation. En annan förenkling är att behandla det kvantmekaniska tunneleringsproblemet som en klassisk process, en slumpvandring. Trots de här grova approximationerna visar hopptransportmodellen ändå många av de fenomen som uppträder i de verkliga materialen som man vill modellera. Man kan kanske säga att hopptransportmodellen är den enklaste modell för oordnade material som fortfarande är intressant att studera.

Man har inte hittat exakta analytiska lösningar för hopptransportmodellen, därför använder man approximationer och numeriska metoder, ofta i form av datorberäkningar. Vi har använt både analytiska metoder och numeriska beräk-

ningar för att studera olika aspekter av hopptransportmodellen. En viktig del av artiklarna som min avhandling baserar sig på är att jämföra analytiska och numeriska resultat. Min andel av arbetet har främst varit att utveckla de numeriska metoderna och applicera dem på hopptransportmodellen. Därför fokuserar jag på den här delen av arbetet i avhandlingens introduktionsdel.

Ett sätt att studera hopptransportmodellen numeriskt är att direkt utföra en slumpvandringsprocess med ett datorprogram. Genom att föra statisik över slumpvandringen kan man beräkna olika transportegenskaper i modellen. Det här är en så kallad Monte Carlo-metod, eftersom själva beräkningen är en slumpmässig process. I stället för att följa rörelsebanan för enskilda elektroner, kan man beräkna sannolikheten vid jämvikt för att hitta en elektron i olika tillstånd. Man ställer upp ett system av ekvationer, som relaterar sannolikheterna för att hitta elektronen i olika tillstånd i systemet med flödet, strömmen, mellan de olika tillstånden. Genom att lösa ekvationssystemet fås sannolikhetsfördelningen för elektronerna. Från sannolikhetsfördelningen kan sedan strömmen och materialets transportegenskaper beräknas.

En aspekt av hopptransportmodellen som vi studerat är elektronernas diffusion, d.v.s. deras slumpmässiga rörelse. Om man betraktar en samling elektroner, så sprider den med tiden ut sig över ett större område. Det är känt att diffusionshastigheten beror av elfältet, så att elektronerna sprider sig fortare om de påverkas av ett elektriskt fält. Vi har undersökt den här processen, och visat att beteendet är väldigt olika i endimensionella system, jämfört med två- och tredimensionella. I två och tre dimensioner beror diffusionskoefficienten kvadratiskt av elfältet, medan beroendet i en dimension är linjärt.

En annan aspekt vi studerat är negativ differentiell konduktivitet, d.v.s. att strömmen i ett material minskar då man ökar spänningen över det. Eftersom det här fenomenet har uppmätts i organiska minnesceller, ville vi undersöka om fenomenet också kan uppstå i hopptransportmodellen. Det visade sig att det i modellen finns två olika mekanismer som kan ge upphov till negativ differentiell konduktivitet. Dels kan elektronerna fastna i fällor, återvändsgränder i systemet, som är sådana att det är svårare att ta sig ur dem då elfältet är stort. Då kan elektronernas medelhastighet och därmed strömmen i materialet minska med ökande elfält. Elektrisk växelverkan mellan elektronerna kan också leda till samma beteende, genom en så kallad coulombblockad. En coulombblockad kan uppstå om antalet ledningselektroner i materialet ökar med ökande spänning. Elektronerna repellerar varandra och ett större antal elektroner kan leda till att transporten blir långsammare, d.v.s. att strömmen minskar.